# Spin Waves in Canted Phases: An Application to Doped Manganites

*José María Román*

*Department of Physics, Loomis Laboratory*

*University of Illinois at Urbana-Champaign*

*1110 W. Green St., Urbana, IL 61801-3080, USA*

*Joan Soto*

*Departament d'Estructura i Constituents de la Matèria and IFAE*

*Universitat de Barcelona*

*Diagonal, 647, E-08028 Barcelona, Catalonia, Spain.*

*e-mails:* romanfau@uiuc.edu, soto@ecm.ub.es

January 3, 2014

**Abstract**

We present the effective lagrangian for low energy and momentum spin waves in canted phases at next to leading order in the derivative expansion. The symmetry breaking pattern $SU(2) \to 1$ of the internal spin group and that of the crystallographic space group imply that there is one ferromagnetic and one antiferromagnetic spin wave. The interaction of the spin waves with the charge carriers is also discussed for canted, ferromagnetic and antiferromagnetic phases. All this together allows us to write the doping dependence of the dispersion relation parameters for doped manganites. We point out that the spin waves posses distinctive characteristics which may allow us to experimentally differentiate canted phases from phase separation regions in doped manganites.

PACS: 75.30.Ds, 75.25.+z, 11.30.Qc, 12.39.Fe

cond-mat/9911471

UB-ECM-PF 98/19

# 1 Introduction

Canted phases are magnetically ordered states with non-collinear magnetisations. These configurations appear in quantum Hall double-layer systems [1] and in the conducting regime of double exchange models [2, 3, 4], where the local magnetisations arrange in two sublattices with magnetizations pointing to different (but not opposite) directions. The double exchange models are believed to provide a good description of doped manganites [5], which are receiving quite a lot of attention lately [6, 7, 8, 9, 10, 11, 12, 13]. Doped manganites present a non-trivial interplay between their magnetic and conducting properties [14, 15, 16, 17, 18, 19], which leads to a rich phase diagram. The transitions between the different phases in terms of the doping have been extensively studied [20].

The most studied transition is that from an antiferromagnetic insulating phase, at zero doping, to a ferromagnetic conducting phase as the doping grows [21]. It is not clear yet if the region for intermediate values of doping corresponds to a canted phase or to a phase separation region [4, 22, 23, 24, 25]. It is our claim that the study of the spin waves in such materials may shed light to this question. Since the spin waves are low energy excitations in a magnetically ordered material, they are sensible to the main features of the phase diagram. The spin waves have indeed been studied recently in connection with these materials [26, 27, 28, 29, 30, 31, 32, 33].

The low energy and momentum dynamics of the spin waves is so much constrained by the symmetries of the system that a model independent description is possible in terms of a few unknown parameters. For canted phases, the spontaneous symmetry breaking pattern of the (internal) spin symmetry is $SU(2) \to 1$, instead of $SU(2) \to U(1)$ like in ferromagnets or antiferromagnets. (Strictly speaking the symmetry breaking pattern is $SU(2) \to Z_2$, the center of the group. However, since we will not be concerned with global properties, neither of the group nor of the coset manifolds, using 1 instead of $Z_2$ does not modify our discussion at all). As a consequence of the Goldstone's theorem there will be gapless excitations in the spectrum (Goldstone modes) [34, 35], the so called spin waves. A very efficient way to encode the spin waves dynamics is by using effective lagrangians.

Effective lagrangians for Goldstone modes are known since the late 1960s [36], and they have been extensively used in pion physics during the last decade [37]. It was suggested in ref. [38] that they may also be useful in Condensed Matter systems. A detailed construction of the effective lagrangians for ferromagnetic and antiferromagnetic spin waves has already been presented in [39] (see [40] for a recent review and [41, 42] for non-trivial applications).

A general formalism for the spin waves in canted phases is presented in Section 2, where we construct an effective lagrangian at next to leading order. An intuitive separation of the spin wave field in one ferromagnetic and one antiferromagnetic component is also presented.

Since canted phases appear in the conducting regime of doped manganites, the coupling of spin waves to charge carriers is relevant. This is discussed in Section 3, where we obtain an effective lagrangian for this coupling in the three different phases: canted, ferromagnetic and antiferromagnetic. In Section 4 we use the previous results for the different phases of doped manganites in order to obtain the explicit dependence of the dispersion relation parameters on the doping, which is given in formulas (4.19), (4.21) and (4.22) for the canted, ferromagnetic and antiferromagnetic phases respectively. In Section 5 we present a plot of the doping dependence of the velocity and the mass of the spin waves for the different phases. We also explain in Section 5 how our results on spin waves can be used to experimentally disentangle canted phases from phase separation regions. We summarize our conclusions in the last section. Some properties and calculations, related to a loop integral, are relegated to the Appendix in order to keep our arguments clear.

In order to simplify the notation we take $\hbar = c = 1$, which leads to a relativistic notation. Hence, we use $x = (t, \mathbf{x})$, $q = (\omega, \mathbf{k})$ and subindices $\mu = 0, 1, 2, 3$, where the zero stands for the time component. Space indices are denoted by $i = 1, 2, 3$.

# 2 Effective Lagrangian for Canted Phases

In a previous paper [22] we obtained the phase diagram for doped manganites, where a rich set of magnetically ordered phases appeared. The magnetically ordered configurations break spontaneously the $SU(2)$ symmetry of the theory (the continuum double exchange model) down to the ground state symmetry, $U(1)$ for the ferromagnetic and antiferromagnetic configuration, and 1 for the canted configuration, because of the non-collinear character of the latter. In this situation the lower excitations of the system are the spin waves, which turn out to be the Goldstone's modes associated to the spontaneous symmetry breaking in magnetic systems.

We have already carried out an extensive study for the ferromagnetic and antiferromagnetic spin waves in crystalline solids in [39]. This formalism assumes the existence of a gap in the excitation spectrum, which permits the construction of an effective lagrangian for the spin waves as an expansion of local terms suppressed by the gap. In the case that there are additional degrees of freedom with energy smaller than the gap, they should also be included in the effective lagrangian. This is the case of charged carriers in doped manganites, which we will discuss in section 3. In this section, we restrict ourselves to the generalization of the formalism presented in [39] to the case of spin waves in canted phases.

## 2.1 Effective fields and symmetries

The (internal) spin symmetry breaking pattern, $SU(2) \to 1$ for the non-collinear canted configurations, determines that the basic field which represents the Goldstone modes (spin waves) may be chosen as a matrix $V(x) \in SU(2)/1 = SU(2)$ [36]. After determining the transformations of this field under the symmetry group of the system we can build an effective lagrangian from which the spin wave dynamics can be derived. The transformations under the $SU(2)$ spin symmetry read

$$V(x) \;\; \to \;\; gV(x) \quad , \quad g \in SU(2). \tag{2.1}$$

The transformations under the crystallographic space group reduce in the continuum to the primitive translations and the point group. Since the local magnetizations in the canted phase point to two different directions depending on the site, both of these symmetries are broken by the ground state. This must be reflected in the transformation properties of $V(x)$. For definiteness, we shall take the local magnetizations in the $1-3$ plane in the spin space, in such a way that the even and odd lattice magnetizations form an angle of $\theta/2$ and $-\theta/2$ with the 3-axis respectively, and can be mapped into each other by a rotation of $\pi$ around the 3-axis.

$$\begin{aligned} \mathbf{M}_1 &= M\left(\sin(\theta/2), 0, \cos(\theta/2)\right) \\ \mathbf{M}_2 &= M\left(-\sin(\theta/2), 0, \cos(\theta/2)\right) \end{aligned} \tag{2.2}$$

For simplicity, we shall also assume a primitive cubic lattice ($Pm\bar{3}m$) although the analysis can be carried out in a similar way for any crystallographic space group. The point group $m\bar{3}m$ is generated by the transformations $C_{2z}$, $C_{2y}$, $C_{2a}$ (a 2-fold axis in the direction $(1,1,0)$), $C_{31}^{+}$ (a 3-fold axis in the direction $(1,1,1)$) and the spatial inversion $I$. These transformations can be separated in two groups, on the one hand $\{C_{2z}, C_{2y}, C_{31}^{+}\}$, which transform points inside each sublattice, and on the other $\{C_{2a}, I\}$, which as the primitive translations, $\tau$, transform points from the even sublattice to the odd one and vice-versa. Thus the transformation of the spin wave field $V(x)$ under this group is given by:

$$\begin{aligned} \xi : \{C_{2z}, C_{2y}, C_{31}^{+}\} : \;\; V(x) &\to g_\xi V(x) \\ \xi : \{C_{2a}, I\} : \;\; V(x) &\to g_\xi V(x) R \quad , \quad R = e^{-i\pi S^3}, \\ \tau : \;\; V(x) &\to V(x) R \end{aligned} \tag{2.3}$$

where $g_\xi$ is the $SU(2)$ transformation associated to the point group transformation and $R$ is a matrix which interchanges the magnetisation between sublattices.

Notice that by combining the transformation of the field $V(x)$ under $\{C_{2a}, I\}$ with the translations in $\{\tau C_{2a}, \tau I\}$ we can eliminate the additional factor $R$ in those point group

transformations. Since, in addition, the factor $g_\xi$ can be re-absorbed by a $SU(2)$ transformation we only have to care about the transformations of the derivatives as far as the point group is concerned.

Finally, under time reversal $V(x)$ transforms as

$$T: \quad V(x) \quad \rightarrow \quad V(x)C \quad , \quad C = e^{-i\pi S^2}. \tag{2.4}$$

We are now in a position to construct the effective lagrangian order by order in derivatives. In order to do that we consider the following element of the Lie algebra of $SU(2)$ [36]:

$$V^\dagger(x) i\partial_\mu V(x) \quad = \quad b_\mu^-(x) S_+ + b_\mu^+(x) S_- + b_\mu^3(x) S^3. \tag{2.5}$$

This term, and consequently the coefficients $b_\mu^a(x)$, are invariant under the $SU(2)$ transformations (2.1). Under the point group we only need to consider the transformation of the derivatives in $b_\mu^a(x)$, which correspond to the space-time indices $\mu$. The transformations under primitive translations are given by

$$\tau: \quad \left\{ \begin{array}{lcl} b_\mu^- & \rightarrow & -b_\mu^- \\ b_\mu^3 & \rightarrow & b_\mu^3, \end{array} \right. \tag{2.6}$$

and under time reversal

$$T: \quad \left\{ \begin{array}{lcl} b_\mu^- & \rightarrow & -b_{t\mu}^+ \\ b_\mu^3 & \rightarrow & -b_{t\mu}^3, \end{array} \right. \tag{2.7}$$

where $t\mu$ stands for the transformation of the index $\mu$ under time reversal $T$.

## 2.2 Relation with ferro and antiferromagnetic spin waves

Before writing down the effective lagrangian, let us discuss a suitable decomposition of $V(x)$ which illuminates the relation between canted spin waves and the usual ferromagnetic and antiferromagnetic ones. In the way we have chosen the direction of the magnetizations in each sublattice (2.2), it is clear that the projection on the third direction is ferromagnetic, whereas the projection on the $1-2$ plane is antiferromagnetic. This suggests that we may separate the spin wave field into components perpendicular to the third axis and to the plane $1-2$ respectively. Group theory allows us to implement this easily. Indeed, an element of the group, $V(x) \in SU(2)$, admits a unique decomposition in terms of an element of a coset, $U(x) \in SU(2)/U(1)$, and an element of the corresponding subgroup, $H(x) \in U(1)$, such that $V(x) = U(x)H(x)$, with

$$\begin{aligned} U(x) \quad &= \quad \exp\left\{ \frac{i}{f_\pi} \left[ \pi^-(x) S_+ + \pi^+(x) S_- \right] \right\} \quad \in \quad SU(2)/U(1) \\ H(x) \quad &= \quad \exp\left\{ \frac{i\sqrt{2}}{f_3} \pi^3(x) S^3 \right\} \quad \in \quad U(1), \end{aligned} \tag{2.8}$$

where $S_\pm = S^1 \pm iS^2$ and $S^3$ are the $SU(2)$ generators, $\pi^\pm(x) = (\pi^1(x) \pm i\pi^2(x))/\sqrt{2}$ and $\pi^3(x)$ are the spin waves fields, and $f_\pi$ and $f_3$ are dimensionful parameters representing the spin stiffness. This implies that the element of the Lie algebra in (2.5) can be written as

$$V^\dagger(x) i\partial_\mu V(x) = H^\dagger(x)(U^\dagger(x) i\partial_\mu U(x))H(x) + H^\dagger(x) i\partial_\mu H(x). \tag{2.9}$$

Upon using for $U^\dagger(x) i\partial_\mu U(x)$ a similar expression to that in (2.5) [39] we have,

$$U^\dagger(x) i\partial_\mu U(x) = a^-_\mu(x) S_+ + a^+_\mu(x) S_- + a^3_\mu(x) S^3. \tag{2.10}$$

This decomposition translates to the coefficients $b^a_\mu(x)$ in (2.5) as follows:

$$\begin{aligned} b^-_\mu(x) &= e^{-i\sqrt{2}\pi^3(x)/f_3} a^-_\mu(x) \\ b^+_\mu(x) &= e^{i\sqrt{2}\pi^3(x)/f_3} a^+_\mu(x) \\ b^3_\mu(x) &= a^3_\mu(x) - \sqrt{2}\partial_\mu \pi^3(x)/f_3. \end{aligned} \tag{2.11}$$

Recall finally that the expansion of $U^\dagger i\partial_\mu U$ in spin wave fields reads

$$U^\dagger i\partial_\mu U = -\frac{1}{f_\pi^2}\left[(f_\pi \partial_\mu \pi^- + \cdots) S_+ + (f_\pi \partial_\mu \pi^+ + \cdots) S_- + (i(\pi^+ \partial_\mu \pi^- - \pi^- \partial_\mu \pi^+) + \cdots) S^3\right]. \tag{2.12}$$

## 2.3 Effective lagrangian

In order to construct the effective lagrangian let us begin by considering terms with time derivatives. It is then clear that we can build a term with a single time derivative,

$$b^3_0 = a^3_0 - \frac{\sqrt{2}}{f_3}\partial_0 \pi^3 \sim a^3_0, \tag{2.13}$$

which contributes to the dynamics of $\pi^\pm(x)$. Nevertheless since this term only contains a total derivative on $\pi^3(x)$ the first contribution to the dynamics of this field comes from

$$b^3_0 b^3_0 \sim \frac{2}{f_3^2}\partial_0 \pi^3 \partial_0 \pi^3, \tag{2.14}$$

where we have made explicit the quadratic term in $\pi^3(x)$.

Regarding the spatial derivatives there are no invariant terms with a single spatial derivative. Then the first invariant terms have two space derivatives, and they read

$$\begin{aligned} & b^+_i b^-_i = a^+_i a^-_i \\ & b^+_i b^+_i + b^-_i b^-_i \\ & b^3_i b^3_i \sim \frac{2}{f_3^2}\partial_i \pi^3 \partial_i \pi^3, \end{aligned} \tag{2.15}$$

where again we have made explicit the quadratic dependence on $\pi^3(x)$ in the last term.

Unlike the terms with time derivatives, the terms with spatial derivatives produce a leading order contributions for $\pi^\pm(x)$ and $\pi^3(x)$ at the same order. Let us call it $O(p^2)$. Equations (2.13), (2.14) and (2.15) provide the dispersion relations for the spin waves, which indicate how time derivatives must be counted with respect to space derivatives. Namely, a time derivative on $\pi^\pm(x)$ must be counted as $O(p^2)$, whereas a time derivative on $\pi^3(x)$ must be counted as $O(p)$. This implies that the term $b_0^3 = a_0^3 - \sqrt{2}\partial_0\pi^3/f_3 \sim O(p^2) + O(p)$, i.e., it contains terms of first and second order, which must be taken into account in the construction of the effective lagrangian. This is in fact a remarkable difference with respect to the ferromagnetic and antiferromagnetic case, where each invariant term has a unique size.

Then, putting together all the terms above, the most general effective lagrangian at order $O(p^2)$ we can construct, with the standard normalizations, reads

$$\mathcal{L}(x) = f_\pi^2\left[\frac{1}{2}b_0^3 - Bb_i^-b_i^+ - \frac{C}{2}(b_i^+b_i^+ + b_i^-b_i^-)\right] + f_3^2\left[\frac{1}{4}b_0^3b_0^3 - \frac{v^2}{4}b_i^3b_i^3\right]. \quad (2.16)$$

If we expand it up to three fields, it reads

$$\begin{aligned}\mathcal{L}(x) &= \pi^-i\partial_0\pi^+ - B\partial_i\pi^-\partial_i\pi^+ - \frac{C}{2}(\partial_i\pi^+\partial_i\pi^+ + \partial_i\pi^-\partial_i\pi^-) \\ &+\frac{1}{2}\partial_0\pi^3\partial_0\pi^3 - \frac{v^2}{2}\partial_i\pi^3\partial_i\pi^3 \\ &-\frac{i\sqrt{2}C}{f_3}(\partial_i\pi^+\partial_i\pi^+ - \partial_i\pi^-\partial_i\pi^-)\pi^3 + \frac{i\sqrt{2}v^2f_3}{2f_\pi^2}(\pi^-\partial_i\pi^+ - \pi^+\partial_i\pi^-)\partial_i\pi^3.\end{aligned} \quad (2.17)$$

The first two lines correspond to quadratic terms in the fields, which yield the free propagation of the spin waves and give the dispersion relation for each of them. Whereas these terms lead directly to a wave equation (Klein-Gordon type) for $\pi^3(x)$, as expected for an antiferromagnetic spin wave, the equation for $\pi^\pm(x)$ turns out to be non-diagonal. The off-diagonal terms are due to the existence in the effective lagrangian of the term $(b_i^+b_i^+ + b_i^-b_i^-)$. In the ferromagnetic and antiferromagnetic cases this term does not appear because the unbroken $U(1)$ subgroup prevents it. In order to diagonalize the quadratic $\pi^\pm(x)$ terms, we perform the following Bogolyubov transformation:

$$\pi^+(x) \rightarrow \sqrt{m'B + \frac{1}{2}}\,\pi^+(x) - \sqrt{m'B - \frac{1}{2}}\,\pi^-(x) \quad , \quad \frac{1}{2m'} = \sqrt{B^2 - C^2}. \quad (2.18)$$

In terms of the new variables the lagrangian (2.17) reads

$$\begin{aligned}\mathcal{L}(x) &= \pi^-i\partial_0\pi^+ - \frac{1}{2m'}\partial_i\pi^-\partial_i\pi^+ + \frac{1}{2}\partial_0\pi^3\partial_0\pi^3 - \frac{v^2}{2}\partial_i\pi^3\partial_i\pi^3 \\ &-\frac{i\sqrt{2}C}{f_3}(\partial_i\pi^+\partial_i\pi^+ - \partial_i\pi^-\partial_i\pi^-)\pi^3 + \frac{i\sqrt{2}v^2f_3}{2f_\pi^2}(\pi^-\partial_i\pi^+ - \pi^+\partial_i\pi^-)\partial_i\pi^3,\end{aligned} \quad (2.19)$$

which yields a Schrödinger equation with a mass $m'$ for the new field $\pi^+(x)$. Therefore, as it was expected from the decomposition made in (2.8)-(2.11) the field $\pi^+(x)$ describes one ferromagnetic spin wave, with a quadratic dispersion relation, and $\pi^3(x)$ describes one antiferromagnetic spin wave, with a linear dispersion relation.

This result is in agreement with previous theoretical [1] and recent experimental [33] works, and in line with the general counting of Goldstone modes in non-relativistic systems stated in [43] (see also [35]). The general statement is that there exist as many real fields representing the Goldstone modes as broken directions in the symmetry group (three in our case, because of the non-collinear nature of the canted configuration). The space-time transformations for these fields determine if they verify a wave (Klein-Gordon, leading to a linear dispersion relation) or a Schödinger (quadratic) equation of motion, with the constraint that in the case of a Schrödinger equation a complex field, and therefore two real ones, is necessary to represent a single physical mode (the two real fields behave like canonical conjugate degrees of freedom). With this argument in mind for the canted spin waves we can only get either three linear branches or one linear and one quadratic branches, which turns out to be the correct answer in our case.

At next to leading order, $O(p^3)$, besides those terms coming from $b_0^3 b_0^3$ already considered in (2.16), we find the following terms:

$$\begin{aligned} &b_0^3 b_0^3 b_0^3 \\ &b_0^3 (b_i^+ b_i^+ + b_i^- b_i^-) \\ &b_0^3 b_i^- b_i^+ \\ &b_0^3 b_i^3 b_i^3. \end{aligned} \tag{2.20}$$

The term $i(b_i^- \partial_0 b_i^+ - b_i^+ \partial_0 b_i^-) \sim b_0^3 b_i^- b_i^+$ at this order, since at $O(p^3)$ we only have to consider time derivative acting on $\pi^3(x)$. However at higher orders the terms obtained from those invariants are different from each other.

### 2.3.1 Coupling to a magnetic field

The most important source of magnetic coupling in a spin system is the Pauli term, the introduction of which in the effective theory was extensibly discussed in [39] . The outcome is that the Pauli term can be introduced by just replacing the time derivative by a covariant derivative in the following way:

$$\partial_0 \longrightarrow D_0 \equiv \partial_0 - i\mu_m \mathbf{SB}. \tag{2.21}$$

After introducing the covariant derivative the equation (2.9), for time derivatives, reads

$$V^\dagger(x) i D_0 V(x) = H^\dagger(x)(U^\dagger(x) i D_0 U(x)) H(x) + H^\dagger(x) i \partial_0 H(x). \tag{2.22}$$

Thus, after introducing the magnetic field the effective lagrangian is constructed with the expressions (2.11) such that the magnetic field only modifies $a_0^{\pm}(x)$ and $a_0^3(x)$, given by

$$\begin{aligned} U^{\dagger} i D_0 U \;=\; & -\frac{1}{f_\pi^2}\left\{\left[f_\pi \partial_0 \pi^- - \mu_m\left(\frac{1}{2}(f_\pi^2 - \pi^+\pi^-)B^{\bar{z}} + \frac{1}{2}\pi^-\pi^- B^z + i f_\pi \pi^- B^3\right) + \cdots\right] S_+ \right. \\ & + \left[f_\pi \partial_0 \pi^+ - \mu_m\left(\frac{1}{2}\pi^+\pi^+ B^{\bar{z}} + \frac{1}{2}(f_\pi^2 - \pi^+\pi^-)B^z - i f_\pi \pi^+ B^3\right) + \cdots\right] S_- \\ & \left. + \left[i(\pi^+\partial_0\pi^- - \pi^-\partial_0\pi^+) - \mu_m\left(i f_\pi \pi^+ B^{\bar{z}} - i f_\pi \pi^- B^z + (f_\pi^2 - 2\pi^+\pi^-)B^3\right) + \cdots\right] S^3\right\}. \end{aligned} \tag{2.23}$$

The time derivative on $\pi^3(x)$, as well as the terms with spatial derivatives $b_i^{\pm}(x)$ and $b_i^3(x)$ remain unchanged by the presence of the magnetic field.

It is very easy to see that, at the lowest order, the dispersion relation of the antiferromagnetic branch, given by $\pi^3(x)$, is not modified by the introduction of a small magnetic field in any direction, in particular in the direction of the staggered magnetization.

### 2.3.2 Ferromagnetic limit

In the ferromagnetic limit the local magnetizations are pointing in the third direction all over the crystal. Hence, an unbroken $U(1)$ symmetry remains, and the spin waves are represented by a field belonging to the coset $SU(2)/U(1)$. This field can be easily obtained from the decomposition (2.9) of the canted case by taking $H(x) = 1$, or, equivalently, $\pi^3(x) = 0$ in (2.11). Hence, $V(x)$ simply reduces to $U(x)$. Furthermore, because of the remaining $U(1)$ symmetry terms like $(a_i^+ a_i^+ + a_i^- a_i^-)$ are forbidden, and hence the quadratic part of the lagrangian does not contain off-diagonal terms. Therefore the Bogolyubov transformation (2.18) is not necessary anymore.

In terms of $a_\mu^a(x)$ the effective lagrangian for the ferromagnetic spin waves reads

$$\mathcal{L}(x) \;=\; f_\pi^2\left[\frac{1}{2}a_0^3 - \frac{1}{2m'}a_i^- a_i^+\right]. \tag{2.24}$$

And after expanding it in terms of spin wave fields in (2.12),

$$\mathcal{L}(x) \;=\; \pi^- i\partial_0\pi^+ - \frac{1}{2m'}\partial_i\pi^-\partial_i\pi^+, \tag{2.25}$$

which corresponds to one spin wave with a quadratic dispersion relation.

### 2.3.3 Antiferromagnetic limit

In the antiferromagnetic limit the local magnetizations are pointing at opposite directions in each sublattice along the first axis ($S^1$). As for the ferromagnetic case an unbroken $U(1)$ symmetry remains, and the spin waves are represented by an element of the coset

$SU(2)/U(1)$. In order to simplify the computation we will rotate the internal space reference frame in such a way that the third direction, instead of the first, lies along the staggered magnetization direction (we perform the rotation $1 \to 3 \to 2$ in all the indices). With this choice the spin wave field is determined from (2.9) by setting $H(x) = 1$, or, equivalently, $\pi^3(x) = 0$ in (2.11). $V(x)$ reduces to $U(x)$, and the remaining $U(1)$ symmetry prevents the non-diagonal terms, $(a_i^+ a_i^+ + a_i^- a_i^-)$, from appearing like in the ferromagnetic case. In addition to that, now $C$ acts as the matrix which interchanges the magnetizations between sublattices, which forbids the term with a single time derivative, $a_0^3(x)$, to appear in the effective lagrangian.

The effective lagrangian for the antiferromagnetic spin waves is given by

$$\mathcal{L}(x) \;=\; f_\pi^2 \left[ a_0^- a_0^+ - v^2 a_i^- a_i^+ \right]. \tag{2.26}$$

And after expanding it in terms of spin wave fields in (2.12),

$$\mathcal{L}(x) \;=\; \partial_0 \pi^- \partial_0 \pi^+ - v^2 \partial_i \pi^- \partial_i \pi^+, \tag{2.27}$$

which describes two spin waves with a linear dispersion relation. These two branches are splitted by the introduction of a small magnetic field in the third direction, the direction of the staggered magnetization [39].

# 3 Interaction with charge carriers

Canted phases are known to support conductivity. Then it is important to elucidate which kind of interaction mediates between the spin waves and the charge carriers. In order to address this question in a model independent way, we would need an effective field theory description of the latter. However, to our knowledge, there are no general rules on how to build such an effective theory, which may depend strongly on the particular material we wish to study. We shall then restrict ourselves to present an effective theory based on a particular model which successfully describes canted phases and has applications to doped manganites, the continuum double exchange model [22].

At first sight one may think of describing the charge carriers by an effective fermion field which varies slowly through the material and couples to the local magnetization. However, in a canted phase the local magnetization changes abruptly from the even to the odd sublattice, which means that we shall need two magnetization fields $\mathbf{M}_1(x)$ and $\mathbf{M}_2(x)$ in the even and odd sublattices, and hence a single slowly varying fermion field is not enough to have a consistent description. We need at least two slowly varying fermion fields $\psi_1(x)$ and $\psi_2(x)$, coupled to the magnetization in the even and odd sublattices respectively.

The interaction lagrangian of the model reads

$$\begin{aligned}\mathcal{L}(x) &= \psi_1^\dagger(x)\left[(1+i\epsilon)i\partial_0+\frac{\partial_i^2}{2m}+\mu+J_H\frac{\boldsymbol{\sigma}}{2}\mathbf{M}_1(x)\right]\psi_1(x)\\ &+\psi_2^\dagger(x)\left[(1+i\epsilon)i\partial_0+\frac{\partial_i^2}{2m}+\mu+J_H\frac{\boldsymbol{\sigma}}{2}\mathbf{M}_2(x)\right]\psi_2(x)\\ &+t\left(\psi_1^\dagger(x)\psi_2(x)+\psi_2^\dagger(x)\psi_2(x)\right),\end{aligned} \tag{3.1}$$

where $t$ corresponds to the amplitude of probability that the fermion changes the sublattice and $J_H$ is the Hund coupling between the fermion fields $\psi_1(x)$ and $\psi_2(x)$ and the magnetic moment in each sublattice $\mathbf{M}_1(x)$ and $\mathbf{M}_2(x)$ respectively. An estimation of our parameters is given by $t\sim zt^l$, $J_H\sim J_H^l$ and $2m\sim 1/a^2t^l$, where $a$ is the lattice spacing, $z=6$ is the coordination number and the superscript $l$ means the analogous lattice quantity. In order to have conduction when $t\neq 0$ only, the chemical potential $\mu$ is required to lie below the lowest energy of the band for $t=0$.

The spin waves are fluctuations of the magnetically ordered ground state, and they are included in the previous fields. We can separate the contribution of the spin waves from that of the ground state $\mathbf{M}_1$ and $\mathbf{M}_2$ by writing $M_i^a(x)=R_b^a(x)M_i^b$ $(i=1,2)$, such that the matrix $R_b^a(x)$ corresponds to the spin wave fluctuation in the adjoint representation of $SU(2)$. Using the scalar product properties the interaction term can be written

$$\frac{\boldsymbol{\sigma}}{2}\mathbf{M}_i(x) \;=\; \frac{\sigma^a}{2}R_b^a(x)M_i^b \;=\; V(x)\frac{\boldsymbol{\sigma}}{2}V^\dagger(x)\mathbf{M}_i \qquad (i=1,2), \tag{3.2}$$

where the matrix $V(x)$ represents the spin waves in the fundamental representation of $SU(2)$.

This expression suggests the following change of variables for the fermionic fields

$$\psi_i(x) \;\longrightarrow\; V(x)\psi_i(x) \qquad (i=1,2). \tag{3.3}$$

In terms of the new fermionic fields the lagrangian (3.1) reads

$$\mathcal{L}(x)=\begin{pmatrix}\psi_1^\dagger(x) & \psi_2^\dagger(x)\end{pmatrix}\left(\hat{O}^{gs}+\hat{O}^{sw}\right)\begin{pmatrix}\psi_1(x)\\ \psi_2(x)\end{pmatrix}, \tag{3.4}$$

where

$$\hat{O}^{gs}=\begin{pmatrix}(1+i\epsilon)i\partial_0+\partial_i^2/2m+\mu+\frac{J_H}{2}\boldsymbol{\sigma}\mathbf{M}_1 & t\\ t & (1+i\epsilon)i\partial_0+\partial_i^2/2m+\mu+\frac{J_H}{2}\boldsymbol{\sigma}\mathbf{M}_2\end{pmatrix} \tag{3.5}$$

is the contribution of the ground state, and

$$\hat{O}^{sw}=\begin{pmatrix}\hat{\mathcal{O}}^{sw} & 0\\ 0 & \hat{\mathcal{O}}^{sw}\end{pmatrix} \quad , \quad \hat{\mathcal{O}}^{sw}=(V^\dagger i\partial_0 V)-\frac{1}{2m}\left[\{i\partial_i,(V^\dagger i\partial_i V)\}+(V^\dagger i\partial_i V)(V^\dagger i\partial_i V)\right], \tag{3.6}$$

contains the interaction with the spin waves. The curly brackets { , } stand for the anti-commutator. Taking into account the decomposition (2.5) the operator $\hat{\mathcal{O}}^{sw}$ can be expressed in terms of the fields $b^a_\mu(x)$ as follows:

$$\begin{aligned}\hat{\mathcal{O}}^{sw} &= \left(b_0^- - \frac{1}{2m}\{i\partial_i, b_i^-\}\right) S_+ + \left(b_0^+ - \frac{1}{2m}\{i\partial_i, b_i^+\}\right) S_- + \left(b_0^3 - \frac{1}{2m}\{i\partial_i, b_i^3\}\right) S^3 \\ &\quad -\frac{1}{2m}\left(b_i^+ b_i^- + \frac{1}{4} b_i^3 b_i^3\right). \end{aligned} \tag{3.7}$$

A compelling expression for the coupling of the spin waves can be written by noting that the expressions (3.4)-(3.7) are equivalent to the introduction of a covariant derivative,

$$i\partial_\mu \longrightarrow iD_\mu = i\partial_\mu + (V^\dagger i\partial_\mu V) = i\partial_\mu + b_\mu^- S_+ + b_\mu^+ S_- + b_\mu^3 S^3, \tag{3.8}$$

in (3.5) and dropping $\hat{\mathcal{O}}^{sw}$.

Since the spin waves are fluctuations of long wavelength and the interaction with the fermionic fields contains derivatives, this interaction will be small. In this situation the problem is reduced to calculate the interaction of the spin waves with the eigenstates of (3.5) perturbatively. The four eigenstates can be obtained by considering the following change of variables:

$$\begin{pmatrix} \psi_1(x) \\ \psi_2(x) \end{pmatrix} = P^\dagger \begin{pmatrix} \chi_1(x) \\ \chi_2(x) \end{pmatrix} \quad , \quad P^\dagger = \frac{1}{\sqrt{2}} \begin{pmatrix} q + Q^\dagger + \bar{Q} & q - Q - \bar{Q} \\ q - Q^\dagger + \bar{Q} & -q - Q + \bar{Q} \end{pmatrix}, \tag{3.9}$$

where $q$ is an scalar parameter and $Q^\dagger$ and $\bar{Q} = \bar{Q}^\dagger$ are matrices in the Lie algebra of $SU(2)$ given by

$$\begin{aligned} q &= \frac{1}{2}\left(\sqrt{\frac{e_+ + \gamma + \cos\frac{\theta}{2}}{2e_+}} + \sqrt{\frac{e_- + \gamma - \cos\frac{\theta}{2}}{2e_-}}\right) \overset{\gamma\ll 1}{\longrightarrow} \frac{1}{2}\left(\cos\frac{\theta}{4} + \sin\frac{\theta}{4}\right) \\ Q^\dagger &= \frac{\sin\frac{\theta}{2}}{\sqrt{2e_-\left(e_- + \gamma - \cos\frac{\theta}{2}\right)}} S_+ + \frac{\sin\frac{\theta}{2}}{\sqrt{2e_+\left(e_+ + \gamma + \cos\frac{\theta}{2}\right)}} S_- \overset{\gamma\ll 1}{\longrightarrow} \cos\frac{\theta}{4} S_+ + \sin\frac{\theta}{4} S_- \\ \bar{Q} &= \left(\sqrt{\frac{e_+ + \gamma + \cos\frac{\theta}{2}}{2e_+}} - \sqrt{\frac{e_- + \gamma - \cos\frac{\theta}{2}}{2e_-}}\right) S^3 \overset{\gamma\ll 1}{\longrightarrow} \left(\cos\frac{\theta}{4} - \sin\frac{\theta}{4}\right) S^3, \end{aligned} \tag{3.10}$$

with

$$e_\pm = \sqrt{1 + \gamma^2 \pm 2\gamma\cos\frac{\theta}{2}} \qquad , \qquad \gamma \equiv \frac{2t}{|J_H| M}, \tag{3.11}$$

$M = |\mathbf{M}_1| = |\mathbf{M}_2| = 3/2$, and $\theta$ the angle formed by the ground state magnetizations $\mathbf{M}_1$ and $\mathbf{M}_2$.

After the change of variables the lagrangian, written in terms of the new fields $\chi_1(x)$ and $\chi_2(x)$, reads

$$\mathcal{L}(x) = \begin{pmatrix} \chi_1^\dagger(x) & \chi_2^\dagger(x) \end{pmatrix} \left[ \begin{pmatrix} \hat{L}_1 & 0 \\ 0 & \hat{L}_2 \end{pmatrix} + \begin{pmatrix} \hat{W}_{11} & \hat{W}_{12} \\ \hat{W}_{21} & \hat{W}_{22} \end{pmatrix} \right] \begin{pmatrix} \chi_1(x) \\ \chi_2(x) \end{pmatrix}, \tag{3.12}$$

where the interaction with the ground state is diagonal, and it is given by

$$\hat{L}_1 = (1+i\epsilon)i\partial_0 + \frac{\partial_i^2}{2m} + \mu + \frac{|J_H|M}{2}\sqrt{1+\gamma^2 \pm 2\gamma\cos\frac{\theta}{2}} \tag{3.13a}$$

$$\hat{L}_2 = (1+i\epsilon)i\partial_0 + \frac{\partial_i^2}{2m} + \mu - \frac{|J_H|M}{2}\sqrt{1+\gamma^2 \mp 2\gamma\cos\frac{\theta}{2}}. \tag{3.13b}$$

The interaction with the spin waves, given by $\hat{W} = P\hat{O}^{sw}P^\dagger$, reads

$$\hat{W}_{11} = q^2\hat{\mathcal{O}}^{sw} + q\{\hat{\mathcal{O}}^{sw}, \bar{Q}\} + \bar{Q}\hat{\mathcal{O}}^{sw}\bar{Q} + Q\hat{\mathcal{O}}^{sw}Q^\dagger \tag{3.14a}$$

$$\hat{W}_{12} = \hat{W}_{21}^\dagger = -q[\hat{\mathcal{O}}^{sw}, Q] - (\bar{Q}\hat{\mathcal{O}}^{sw}Q + Q\hat{\mathcal{O}}^{sw}\bar{Q}) \tag{3.14b}$$

$$\hat{W}_{22} = q^2\hat{\mathcal{O}}^{sw} - q\{\hat{\mathcal{O}}^{sw}, \bar{Q}\} + \bar{Q}\hat{\mathcal{O}}^{sw}\bar{Q} + Q^\dagger\hat{\mathcal{O}}^{sw}Q, \tag{3.14c}$$

where the square brackets [ , ] stand for the commutator and $\hat{\mathcal{O}}^{sw}$ is given in (3.7).

In the relevant materials that we have in mind, the hopping amplitude, $t$, is much smaller than the Hund coupling, $J_H$, i.e. $\gamma \ll 1$. In this case, the two higher states of (3.5), denoted by $\chi_2(x)$, lie far away from the two lower ones. In fact, the ratio of energies is of order $\gamma$. If we are only interested in transition energies $\sim t$ we can safely integrate out the states $\chi_2(x)$, obtaining the following lagrangian for the two lowest states, $\chi_1(x)$:

$$\mathcal{L}_{\mathit{eff}} = \chi_1^\dagger(x)\left(\hat{L}_1 + \hat{W}_{11}\right)\chi_1(x) - \chi_1^\dagger(x)\hat{W}_{12}\frac{1}{\hat{L}_2 + \hat{W}_{22}}\hat{W}_{21}\chi_1(x). \tag{3.15}$$

The second term is of order $\gamma$ with respect to the first one. Indeed, we consider low incoming energy and momentum with respect to the two lowest states, namely, $\hat{L}_1 \sim (1+i\epsilon)i\partial_0 + \partial_i^2/2m + \mu + |J_H|M/2 \sim t$, and the spin wave interaction $\hat{W}_{ij} \sim t$. Thus $1/\hat{L}_2 \sim \gamma/t$, such that the second term in (3.15) is order $\gamma t$, which means that the field $\chi_2(x)$ decouples, and the effective lagrangian reduces to

$$\mathcal{L}_{\mathit{eff}} = \chi_1^\dagger(x)\left(\hat{L}_1 + \hat{W}_{11} + O(\gamma t)\right)\chi_1(x). \tag{3.16}$$

In order to complete the effective lagrangian we must consider the leading order in $\gamma$ for $\hat{W}_{11}$ in (3.14a), which corresponds to take the right limit in (3.10) for the parameter $q$ and the matrices $Q^\dagger$ and $\bar{Q}$.

Therefore, the effective lagrangian is given by (3.16), where the interaction terms, which come from (3.14a), (3.7) and (3.10), are given by

$$\begin{aligned}\hat{W}_{11} &= -\frac{1}{2m}\left(b_i^+ b_i^- + \frac{1}{4}b_i^3 b_i^3\right) + \frac{1}{2}\cos\frac{\theta}{2}\left(b_0^3 - \frac{1}{2m}\{i\partial_i, b_i^3\}\right) \\ &\quad + \frac{1}{2}\sin\frac{\theta}{2}\left(b_0^- - \frac{1}{2m}\{i\partial_i, b_i^-\} + b_0^+ - \frac{1}{2m}\{i\partial_i, b_i^+\}\right)(S_+ + S_-)\,. \end{aligned} \tag{3.17}$$

Upon expanding it up to two fields, using (2.12) and (2.11), we finally obtain

$$\begin{aligned}\hat{W}_{11} &= -\frac{1}{2mf_\pi^2}\left[\partial_i\pi^-\partial_i\pi^+ + \frac{f_\pi^2}{2f_3^2}\partial_i\pi^3\partial_i\pi^3\right] \\ &\quad + \frac{1}{2f_\pi^2}\cos\frac{\theta}{2}\Bigg[\pi^-\left(i\partial_0\pi^+ + \frac{1}{2m}\{\partial_i, \partial_i\pi^+\}\right) - \pi^+\left(i\partial_0\pi^- + \frac{1}{2m}\{\partial_i, \partial_i\pi^-\}\right) \\ &\qquad + \frac{i\sqrt{2}f_\pi^2}{f_3}\left(i\partial_0\pi^3 + \frac{1}{2m}\{\partial_i, \partial_i\pi^3\}\right)\Bigg] \\ &\quad + \frac{1}{2f_\pi f_3}\sin\frac{\theta}{2}\Bigg[if_3\left(i\partial_0\pi^- + i\partial_0\pi^+ + \frac{1}{2m}\{\partial_i, \partial_i\pi^- + \partial_i\pi^+\}\right) \\ &\qquad + \sqrt{2}\pi^3\left(i\partial_0\pi^- - i\partial_0\pi^+ + \frac{1}{2m}\{\partial_i, \partial_i\pi^- - \partial_i\pi^+\}\right) \\ &\qquad + \frac{\sqrt{2}}{2m}\partial_i\pi^3(\partial_i\pi^- - \partial_i\pi^+)\Bigg](S_+ + S_-)\,. \end{aligned} \tag{3.18}$$

## 3.1 Coupling to ferromagnetic spin waves

The interaction of charge carriers with ferromagnetic spin waves can be considered as a limit of the canted configuration. In order to do that we must take the limit $\theta \to 0$ in (3.10), which yields a very simple expression, independent of $\gamma$, for the parameter $q$ and the matrices $Q^\dagger$ and $\bar{Q}$ which determine the change of variables (3.9), namely,

$$q \;=\; \frac{1}{2} \qquad\qquad Q^\dagger \;=\; S_+ \qquad\qquad \bar{Q} \;=\; S^3. \tag{3.19}$$

Following the considerations in subsection 2.3.1, we also must take $H(x) = 1$, or equivalently $\pi^3(x) = 0$.

Because of the remaining unbroken symmetry the $SU(2)$ transformations on the spin wave fields are realized by a non-linear $U(1)_{local}$ gauge group, which allows us to write the lagrangian in a manifestly gauge invariant way

$$\hat{L}_1 + \hat{W}_{11} = iD_0 + \frac{1}{2m}\left(D_iD_i - a_i^-a_i^+\right) + \mu + \frac{|J_H|M}{2} + 2tS^3, \tag{3.20}$$

where $iD_\mu = i\partial_\mu + a_\mu^3/2$. Notice that this implies that some of the couplings are fixed by the symmetry. In fact only the coupling $a_i^-a_i^+$ is model dependent. This is analogous to

what happens in the pion-nucleon lagrangian where one of the couplings is fixed by chiral symmetry [44]. Recall that the transformation properties under $U(1)_{local}$ are the following:

$$\begin{aligned} \chi_i(x) &\longrightarrow e^{i\frac{\varphi(x)}{2}}\chi_i(x) \\ a_\mu^\pm(x) &\longrightarrow e^{\mp i\varphi(x)}a_\mu^\pm(x) \\ a_\mu^3(x) &\longrightarrow a_\mu^3(x)+\partial_\mu\varphi(x). \end{aligned} \tag{3.21}$$

Finally, in terms of the spin wave fields and up to two fields $\hat{W}_{11}$ reads

$$\begin{aligned} \hat{W}_{11} &= -\frac{1}{2mf_\pi^2}\partial_i\pi^-\partial_i\pi^+ \\ &\quad +\frac{1}{2f_\pi^2}\left[\pi^-\left(i\partial_0\pi^+ +\frac{1}{2m}\{\partial_i,\partial_i\pi^+\}\right)-\pi^+\left(i\partial_0\pi^- +\frac{1}{2m}\{\partial_i,\partial_i\pi^-\}\right)\right], \end{aligned} \tag{3.22}$$

which corresponds to the limit $\theta\to 0$ of the canted expression (3.18).

## 3.2 Coupling to antiferromagnetic spin waves

In the antiferromagnetic case we have to consider two situations. The first one corresponds to the insulating phase, where there are no charge carriers to couple with. The second situation corresponds to the antiferromagnetic conducting phase. We shall describe this second situation below.

The interaction of the charge carriers with antiferromagnetic spin waves is given by the canted case in the limit $\theta\to\pi$. According to the discussion in subsection 2.3.2 this limit is a little bit more involved than for the ferromagnetic case, since we also must rotate the reference system ($1\to 3\to 2$). Then the expressions for the parameter $q$ and the matrices $Q^\dagger$ and $\bar{Q}$, which determine the change of variables (3.9), read

$$\begin{aligned} q &= \frac{1}{\sqrt{2}}\sqrt{1+\frac{\gamma}{\sqrt{1+\gamma^2}}} \overset{\gamma\ll 1}{\longrightarrow} \frac{1}{\sqrt{2}} \\ Q^\dagger &= \sqrt{\frac{2}{1+\gamma^2+\gamma\sqrt{1+\gamma^2}}}\,S^3 \overset{\gamma\ll 1}{\longrightarrow} \sqrt{2}S^3 \\ \bar{Q} &= 0, \end{aligned} \tag{3.23}$$

where the right limit gives the leading dependence on $\gamma$ which we shall use to calculate the interaction.

Similarly to the ferromagnetic case we must take $H(x)=1$, or $\pi^3(x)=0$, and therefore the remaining unbroken symmetry determines the gauge invariance structure for the effective lagrangian, given by

$$\hat{L}_1+\hat{W}_{11} = iD_0+\frac{1}{2m}\left(D_iD_i-a_i^-a_i^+\right)+\mu+\frac{|J_H|M}{2}, \tag{3.24}$$

where now $iD_\mu = i\partial_\mu + a_\mu^3 S^3$. Notice again that this implies that some of the couplings are fixed by the symmetry. In fact only the coupling $a_i^- a_i^+$ is model dependent. This is analogous to what happens in the ferromagnetic case discussed before and, hence, also analogous to the case of the pion-nucleon lagrangian [44]. Recall that the transformation properties under $U(1)_{local}$ are now the following:

$$\begin{aligned} \chi_i(x) &\longrightarrow e^{i\varphi(x)S^3}\chi_i(x) \\ a_\mu^\pm(x) &\longrightarrow e^{\mp i\varphi(x)}a_\mu^\pm(x) \\ a_\mu^3(x) &\longrightarrow a_\mu^3(x) + \partial_\mu\varphi(x). \end{aligned} \tag{3.25}$$

Finally, in terms of the spin wave fields and up to two fields $\hat{W}_{11}$ reads

$$\begin{aligned} \hat{W}_{11} &= -\frac{1}{2mf_\pi^2}\partial_i\pi^-\partial_i\pi^+ \\ &\quad + \frac{1}{f_\pi^2}\left[\pi^-\left(i\partial_0\pi^+ + \frac{1}{2m}\{\partial_i,\partial_i\pi^+\}\right) - \pi^+\left(i\partial_0\pi^- + \frac{1}{2m}\{\partial_i,\partial_i\pi^-\}\right)\right]S^3, \end{aligned} \tag{3.26}$$

which corresponds to the limit $\theta \to \pi$ of the canted expression (3.18). However because of the rotation of the reference system it is easier to obtain (3.26) as a limit of (3.17) rather than (3.18), because the direction of the symmetry breaking has not been taken explicitly yet.

# 4 Spin Waves in Doped Manganites

In the section 2 we developed a general formalism which provides the effective lagrangian for the spin waves generated by any model in a canted, ferromagnetic and antiferromagnetic ground state as long as the model is invariant under $SU(2)$ transformations. In this section we are going first to particularize this effective lagrangian to the case of the spin waves in doped manganites. Next, we will include the interaction of spin waves to charge carriers worked out in section 3 and calculate the doping dependence of dispersion relation parameters.

## 4.1 Spin waves from the Heisenberg hamiltonian

In the double exchange models the interaction between the core spins in the $t_{2g}$-bands of the manganese atom is described by an antiferromagnetic hamiltonian. Since the value of the core spins is 3/2 their motion is slow and can be approximated by classical magnetization fields on the lattice. Furthermore, for the low energy and momentum region the lattice fields can be further approximated by continuum fields. In [22] we considered a static Heisenberg-like interaction, which only provides the relevant contribution to the ground state energy.

Here we shall introduce a derivative expansion of the Heisenberg hamiltonian, which also takes care of the low energy and momentum excitations. These derivative terms in the second quantization language read

$$H = -\int d\mathbf{x} \frac{J_{AF} a^2}{2z} \partial_i \mathbf{M}_1(x) \partial_i \mathbf{M}_2(x), \tag{4.1}$$

where $J_{AF} \sim z J^l_{AF}/a^3$ and the superscript $l$ represents the lattice Heisenberg coupling. The local magnetizations for each sublattice, $\mathbf{M}_1(x)$ and $\mathbf{M}_2(x)$, are given as fluctuations of the ground state configuration, as mentioned in section 2, that we can write $\varphi_i(x) = V(x)\varphi^{(0)}_i$,

$$\mathbf{M}_i(x) = \varphi^{(0)\dagger}_i V^\dagger(x) \mathbf{S} V(x) \varphi^{(0)}_i = tr\left(V^\dagger(x) \mathbf{S} V(x) P_i\right) = R^a_b(x) M^b_i, \tag{4.2}$$

where $P_i$ is a projector in the direction of the ground state magnetization in each sublattice $i = 1, 2$.

This hamiltonian only generates terms with spatial derivatives in the spin wave's effective lagrangian. In order to introduce the temporal term let us consider it written in terms of the total, $\mathbf{\Sigma}(x)$, and staggered, $\mathbf{\Omega}(x)$, magnetizations

$$H = -\int d\mathbf{x} \left[ \frac{J_{AF} a^2}{2z} \partial_i \mathbf{\Sigma}(x) \partial_i \mathbf{\Sigma}(x) - \frac{J_{AF} a^2}{8z} \partial_i \mathbf{\Omega}(x) \partial_i \mathbf{\Omega}(x) \right], \tag{4.3}$$

where

$$\begin{aligned} \mathbf{\Sigma}(x) &= \frac{1}{2}\left(\mathbf{M}_1(x) + \mathbf{M}_2(x)\right) & \Sigma &= M \cos\frac{\theta}{2} \\ \mathbf{\Omega}(x) &= \mathbf{M}_1(x) - \mathbf{M}_2(x) & \Omega &= 2M \sin\frac{\theta}{2}. \end{aligned} \tag{4.4}$$

This corresponds to the spatial derivatives terms in the effective lagrangian for ferromagnetic spin waves in terms of the total magnetization, $\mathbf{\Sigma}(x)$, and for antiferromagnetic spin waves in terms of the staggered magnetization, $\mathbf{\Omega}(x)$, [45]. Following this identification we shall choose as temporal terms those which complete these hamiltonians. Then the effective lagrangian from the Heisenberg contribution reads

$$\begin{aligned} \mathcal{L}^{(1)}(x) &= \frac{1}{a^3 \Sigma^2} \int_0^1 d\lambda \mathbf{\Sigma}(x,\lambda) \left(\partial_0 \mathbf{\Sigma}(x,\lambda) \times \partial_\lambda \mathbf{\Sigma}(x,\lambda)\right) + \frac{J_{AF} a^2}{2z} \partial_i \mathbf{\Sigma}(x) \partial_i \mathbf{\Sigma}(x) \\ &\quad + \frac{z}{12 J_{AF} a^6 \Omega^2} \left[ \frac{1}{2} \partial_0 \mathbf{\Omega}(x) \partial_0 \mathbf{\Omega}(x) - \frac{3 J^2_{AF} a^8 \Omega^2}{2z^2} \partial_i \mathbf{\Omega}(x) \partial_i \mathbf{\Omega}(x) \right], \end{aligned} \tag{4.5}$$

where $\mathbf{\Sigma}(x,\lambda)$ is an extension of the total magnetization field which verifies $\mathbf{\Sigma}(x,0) = \mathbf{\Sigma}$ and $\mathbf{\Sigma}(x,1) = \mathbf{\Sigma}(x)$. This is equivalent to introduce an extension $\pi^a(x,\lambda)$ for the spin wave fields such that $\pi^a(x,0) = 0$ and $\pi^a(x,1) = \pi^a(x)$. A simple extension valid for our

purposes is $\pi^a(x,\lambda) = \lambda\pi^a(x)$, which allows us to write the effective lagrangian for the canted configuration in terms of the spin wave representation used in section 2,

$$\begin{aligned}\mathcal{L}^{(1)}(x) &= \frac{2\Sigma}{a^3}\left[\frac{1}{2}b_0^3 + \frac{J_{AF}a^5}{8z\Sigma}(8\Sigma^2-\Omega^2)b_i^-b_i^+ + \frac{J_{AF}a^5\Omega^2}{8z\Sigma}(b_i^+b_i^+ + b_i^-b_i^-)\right] \\ &\quad + \frac{z}{6J_{AF}a^6}\left[\frac{1}{4}b_0^3b_0^3 - \frac{3J_{AF}^2a^8\Omega^2}{4z^2}b_i^3b_i^3\right]. \end{aligned} \tag{4.6}$$

We have dropped terms with two time derivatives acting on $\pi^{\pm}(x)$ since they are subleading in the canted and ferromagnetic phases. However, they are not so in the antiferromagnetic phase and will have to be restored in order to take the antiferromagnetic limit. Notice that (4.6) provides particular values for the constants $f_\pi^2$, $B$, $C$, $f_3^2$ and $v^2$ in the general formula (2.16).

### 4.1.1 Ferromagnetic configuration

In the case we have the ferromagnetic configuration the limit is taken very easily, since in this case $\Sigma \to M$ and $\Omega \to 0$. Since the time evolution is already described by the term with a single time derivative we can drop the two time derivatives term in (4.6), which yields the effective lagrangian

$$\mathcal{L}^{(1)}(x) = \frac{2M}{a^3}\left[\frac{1}{2}a_0^3 + \frac{J_{AF}a^5M}{z}a_i^-a_i^+\right]. \tag{4.7}$$

Notice that the mass term in (4.7) has the wrong sign. This is due to the fact that (4.7) has been derived from an antiferromagnetic Heisenberg hamiltonian. Although this wrong sign apparently produces an instability in the ferromagnetic spin wave spectrum, this instability is not significant. Recall that the ferromagnetic phases in doped manganites are due to the interaction with the charge carriers. Hence any reliable estimate of the spin wave dispersion relation parameters in the ferromagnetic phase must also take into account the interaction with the charge carriers. We shall do so later on. Such kind of (fictitious) instabilities also occur in the canted phases although they are not so immediately spotted from the Lagrangian (4.6).

### 4.1.2 Antiferromagnetic configuration

In the antiferromagnetic configuration $\Sigma \to 0$ and $\Omega \to 2M$, and after performing the corresponding rotation, $1 \to 3 \to 2$, as explained in section 2, we obtain the following effective lagrangian:

$$\mathcal{L}^{(1)}(x) = \frac{z}{6J_{AF}a^6}\left[a_0^-a_0^+ - \frac{12J_{AF}^2a^8M^2}{z^2}a_i^-a_i^+\right]. \tag{4.8}$$

In this case, since the ground state configuration is supported by the Heisenberg hamiltonian, the spin waves obtained from it are stable.

## 4.2 Spin waves dispersion relations: contributions from charge carriers

We have now at our disposal suitable low energy effective lagrangians which describe spin waves in doped manganites in the canted, ferromagnetic and antiferromagnetic phases. They are given by the pure spin wave terms above together with the terms of interaction with the charge carriers (3.16). More precisely, the effective lagrangian for the canted phases can be obtained from (3.16), (3.17) and (4.6), for the ferromagnetic phase from (3.16), (3.20) and (4.7), and for the antiferromagnetic phase from (3.16), (3.24) and (4.8).

In order to obtain a reliable evaluation of the parameters in the spin waves dispersion relations we have to take into account the interaction with the charge carriers in the spin waves two point Green's functions. This can be easily achieved from a further (this time non-local) effective lagrangian which is obtained by integrating out the charge carriers and keeping only the contributions up to two spin wave fields.

By integrating out the fermionic fields in the equation (3.16) we obtain the following contributions to the effective lagrangian:

$$S^{(2)}_{eff} = -iTr\log(\hat{L}_1+\hat{W}_{11}) = -iTr\log\hat{L}_1 - iTr(\hat{L}_1^{-1}\hat{W}_{11}) + \frac{i}{2}Tr(\hat{L}_1^{-1}\hat{W}_{11}\hat{L}_1^{-1}\hat{W}_{11}) + \cdots, \quad (4.9)$$

where $Tr$ stands for the trace over the space-time indices as well as the matrix indices. We have expanded the logarithm up to second order.

The first term in (4.9) gives rise to an effective potential for the ground state configuration which, together with the static antiferromagnetic Heisenberg term, produces the rich phase diagram for doped manganites presented in [22]. The following two terms in the expansion are responsible for the appearance of terms with at least two spin waves in the effective lagrangian, as can be see from (3.18).

Even though in order to obtain the relevant contributions to the effective lagrangian it is enough to consider the interaction up to two spin waves in (3.18), interesting general characteristics will arise if, instead, we use the $SU(2)$ invariant expression (3.17) for the interaction. In this way we are going to obtain not only an explicitly invariant effective lagrangian under $SU(2)$, but also the non-local structure which arises from the absence of gap in the fermionic spectrum of excitation.

We begin with the calculation of the second term in (4.9), i.e. $S^{(2,1)}_{eff} = -iTr(\hat{L}_1^{-1}\hat{W}_{11})$. In this calculation a closed loop integral, representing the density of carriers, appears,

$$\frac{x}{a^3} = -i\int_{-\infty}^{\infty}\frac{d\omega}{2\pi}\frac{d\mathbf{k}}{(2\pi)^3}trL_1^{-1}(q)e^{i\omega\eta}. \quad (4.10)$$

$x$ is the doping and $a^3$ the volume of the unit cell. $tr$ represents the matrix trace, the space-time trace has already been taken into account in the integration over the momentum $q = (\omega, \mathbf{k})$. $L_1^{-1}(q)$ is the Fourier transform of the inverse of the operator $\hat{L}_1$ given in (3.13a). The convergence factor $e^{i\omega\eta}$ ($\eta \to 0^+$) is introduced to pick up the correct order of the fields in the calculation of closed loops of one point Green's functions [46].

The contribution of these terms to the effective lagrangian is given by

$$\mathcal{L}^{(2,1)}(u) = \frac{x}{2a^3}\cos\frac{\theta}{2}\; b_0^3 - \frac{x}{2ma^3}\left[b_i^- b_i^+ + \frac{1}{4} b_i^3 b_i^3\right], \tag{4.11}$$

where we have dropped terms which contribute with a total derivative.

Whereas all the contributions in (4.11) are local, because the loop integral is closed, the contribution from $S_{eff}^{(2,1)} = \frac{i}{2} Tr(\hat{L}_1^{-1}\hat{W}_{11}\hat{L}_1^{-1}\hat{W}_{11})$ is going to contain non-local terms due to the presence of the so-called vacuum polarization tensor

$$\Pi_{ab}^{(i,j)}(p) = -i\int \frac{dq}{(2\pi)^4}\; (p+q)^i L_{1a}^{-1}(p+q)\; q^j L_{1b}^{-1}(q), \tag{4.12}$$

where $a, b = +, -$ represent the diagonal components of the operator $\hat{L}_1$ given in (3.13a). $i, j = 1, 2, 3$ represent the spatial components of the momentum, while $i, j = 0$ means the absence of the corresponding momentum component. The properties of this tensor are displayed in the Appendix.

Taking into account the symmetry properties of the vacuum polarization tensor the contribution to the effective lagrangian reads

$$\begin{aligned} S_{eff}^{(2,2)} \;=\; & -\int du dw \int \frac{dp}{(2\pi)^4}\; e^{-ip(u-w)} \\ & \left\{\frac{1}{8}\cos^2\frac{\theta}{2}\left[\Pi_{aa}^{(0,0)}(p)\; b_0^3(u) b_0^3(w) + \frac{2}{m}\Pi_{aa}^{(0,i)}(p)\; b_0^3(u) b_i^3(w) + \frac{1}{m^2}\Pi_{aa}^{(i,j)}(p)\; b_i^3(u) b_j^3(w)\right]\right. \\ & \left. + \frac{1}{4m^2}\sin^2\frac{\theta}{2}\;\Pi_{+-}^{(i,j)}(p)\Big[b_i^-(u) b_j^+(w) + b_i^+(u) b_j^-(w) + b_i^+(u) b_j^+(w) + b_i^-(u) b_j^-(w)\Big]\right\}, \end{aligned} \tag{4.13}$$

where summation convention over repeated indices has been used, and as in the previous case terms contributing with a total derivative to the effective lagrangian have been dropped. It is easy to see that this part contributes with non-local terms as long as the vacuum polarization tensor has a non-constant behavior in the energy-momentum vector $p^\mu = (\nu, \mathbf{p})$. One of the most interesting terms with these characteristics is $b_0^3(u) b_i^3(w)$, which mixes time and spatial derivatives.

The leading contribution to the effective lagrangian is given by keeping in (4.13) second order terms in derivatives (or momentum). This corresponds to consider the zero energy and momentum limit of the vacuum polarization tensor, i.e. $\Pi_{ab}^{(i,j)}(0)$. It is also convenient

to choose the basis (A.4), which has its third component parallel to the momentum, $\mathbf{p}$, in order to simplify the calculation. In this basis, and using the relations given in (A.8) and (A.9), the action (4.13) reads

$$\begin{aligned}
S_{eff}^{(2,2)} &= -\int du dw \int \frac{dp}{(2\pi)^4}\, e^{-ip(u-w)} \Big\{ \frac{1}{8}\cos^2\frac{\theta}{2}\,\Pi_{aa}^{(0,0)}(0) \\
&\qquad \Big[ b_0^3(u)b_0^3(w) + 2\frac{\nu}{|\mathbf{p}|} b_0^3(u)\left(e_{(3)}^i b_i^3(w)\right) + \left(\frac{\nu}{|\mathbf{p}|}\right)^2 \left(e_{(3)}^i b_i^3(u)\right)\left(e_{(3)}^j b_j^3(w)\right)\Big] \\
&\quad - \frac{1}{8}\cos^2\frac{\theta}{2}\,\frac{x}{ma^3}\left(e_{(3)}^i b_i^3(u)\right)\left(e_{(3)}^j b_j^3(w)\right) \\
&\quad + \frac{1}{8}\cos^2\frac{\theta}{2}\,\Pi_{aa}^{(1,1)}(0)\Big[\left(e_{(1)}^i b_i^3(u)\right)\left(e_{(1)}^j b_j^3(w)\right) + \left(e_{(2)}^i b_i^3(u)\right)\left(e_{(2)}^j b_j^3(w)\right)\Big] \qquad (4.14) \\
&\quad + \frac{1}{4m^2}\sin^2\frac{\theta}{2}\,\Pi_{+-}^{(\alpha,\alpha)}(0)\Big[\left(e_{(\alpha)}^i b_i^-(u)\right)\left(e_{(\alpha)}^j b_j^+(w)\right) + \left(e_{(\alpha)}^i b_i^+(u)\right)\left(e_{(\alpha)}^j b_j^-(w)\right) \\
&\qquad + \left(e_{(\alpha)}^i b_i^+(u)\right)\left(e_{(\alpha)}^j b_j^+(w)\right) + \left(e_{(\alpha)}^i b_i^-(u)\right)\left(e_{(\alpha)}^j b_j^-(w)\right)\Big]\Big\}.
\end{aligned}$$

Hence, with the aid of (2.12) and (2.11) we can expand this expression up to two spin waves. At this order only one spin wave must be considered in the expansion of (2.11), i.e. $b_\mu^a \sim \partial_\mu \pi^a$, which means that they are proportional to the energy-momentum, and since the vectors $\hat{\mathbf{e}}_{(1)}$ and $\hat{\mathbf{e}}_{(2)}$ are perpendicular to the momentum, $e_{(\alpha)}^i b_i^a \sim e_{(\alpha)}^i \partial_i \pi^a \sim i e_{(\alpha)}^i p^i \pi^a = 0$, $(\alpha = 1, 2)$, they do not contribute at this order.

In addition to this, it is very interesting to notice how the terms in the second line, which would contribute with time derivatives for $\pi^3(u)$, cancel at this order,

$$\frac{\nu}{|\mathbf{p}|} e_{(3)}^i b_i^3 \sim \frac{\nu p^i}{\mathbf{p}^2}\partial_i \pi^3 \sim i\nu\pi^3 \sim -\partial_0 \pi^3. \qquad (4.15)$$

The cancellation of these terms is very important, since as it can be seen from (A.8) the tensor $\Pi_{aa}^{(0,0)}(0)$ contains an imaginary part, which would produce the spontaneous decay of the spin wave $\pi^3(u)$ into fermionic excitations.

The final result for the effective lagrangian up to two spin waves, after using a similar procedure to (4.15) for spatial derivatives, turns out to be

$$\begin{aligned}
\mathcal{L}^{(2,2)}(u) &= \frac{J_{AF} M^2}{2mtf_\pi^2}\,\Pi_{+-}\sin^2\frac{\theta}{2}\left[\partial_i\pi^-\partial_i\pi^+ + \frac{1}{2}\left(\partial_i\pi^+\partial_i\pi^+ + \partial_i\pi^-\partial_i\pi^-\right)\right] \\
&\quad + \frac{x}{4ma^3 f_3^2}\cos^2\frac{\theta}{2}\,\partial_i\pi^3\partial_i\pi^3, \qquad (4.16)
\end{aligned}$$

where $\Pi_{+-}$ is given in (A.12) and (A.14) for one band canted ($CC1$) and two band canted ($CC2$) phases respectively.

### 4.2.1 Ferromagnetic configuration

The ferromagnetic limit is again very easily taken from the canted results when $\theta \to 0$ (equivalently we could use (3.20)). In addition to that, we notice from (3.22) that the interaction already contains at least two spin waves, thus in order to calculate the dispersion relation we only have to consider the second term in the expansion of the logarithm (4.9). The effective lagrangian at this order is

$$\mathcal{L}^{(2,1)}(u) = \frac{x}{2a^3}\, a_0^3 - \frac{x}{2ma^3} a_i^- a_i^+. \tag{4.17}$$

### 4.2.2 Antiferromagnetic configuration

In the extreme low energy and momentum limit we are interested in, there will be a contribution for the antiferromagnetic state in the conducting phase only. As in the previous cases the antiferromagnetic limit of the canted expression must be taken carefully. In this case, as in the ferromagnetic one, the interaction already contains at least two spin waves and it is enough to consider the second term in (4.9). Since the antiferromagnetic state corresponds to a 2-fold band, $\hat{L}_1$ is degenerated, the term proportional to $S^3$ in (3.24) will cancel, which prevents a term with a single time derivative from appearing in the effective lagrangian as it should be. The final result reads

$$\mathcal{L}^{(2,1)}(u) = -\frac{x}{2ma^3} a_i^- a_i^+. \tag{4.18}$$

## 4.3 Spin waves dispersion relations: final results

Finally by summing all the contributions $\mathcal{L} = \mathcal{L}^{(1)} + \mathcal{L}^{(2,1)} + \mathcal{L}^{(2,2)}$, given in (4.6), (4.11) and (4.16) respectively, we are in the position to write the effective lagrangian for the spin waves up to second order in derivatives, and up to two spin wave fields. After expanding the first two contributions in spin wave fields and taking into account the expression (2.17) we obtain for the parameters of the spin waves the following results:

$$\begin{aligned}
f_\pi^2 &= \frac{2M+x}{a^3}\, y \\
B &= \frac{1}{2m}\frac{z^{3/2}}{15\pi^2 A}\frac{1}{(2M+x)y}\left[(1-3y^2) + \frac{5A}{2}\left(\frac{6\pi^2 x}{z^{3/2}}\right) - \Pi_{+-}(1-y^2)\right] \\
C &= -\frac{1}{2m}\frac{z^{3/2}}{15\pi^2 A}\frac{1}{(2M+x)y}\left[1+\Pi_{+-}\right](1-y^2) \\
f_3^2 &= \frac{z}{6J_{AF}a^6} \\
v^2 &= \frac{6J_{AF}a^3M^2}{2mz}\frac{z^{3/2}}{15\pi^2 A}\frac{1}{M^2}\left[2 + \frac{5A}{2}\left(\frac{6\pi^2 x}{z^{3/2}}\right)\right](1-y^2),
\end{aligned} \tag{4.19}$$

where $y = \cos\theta/2$ is a measure of the canting angle $\theta$ and $x$ is the doping. $\Pi_{+-}$ also depends on $x$. We have used the expression of the parameter $A$ in (A.11) and $2m \sim z/a^2 t$. In the case of the one band canted phase ($CC1$) $\Pi_{+-}$ is given by (A.12), and all the expressions can be written explicitly in terms of the doping using (A.11). In the case of the two band canted phases ($CC2$) $\Pi_{+-}$ is given by (A.14), but it is impossible to write all the above expressions explicitly in terms of the doping only; we need also the canting angle, $y$, which depends implicitly on the doping. For a given value of the doping we can obtain the corresponding value of $y$ by solving the equations (A.13).

As it was described in section 2 a Bogolyubov transformation must be carried out in order to diagonalize the lagrangian and obtain the physical fields, which have a mass given by $1/2m' = \sqrt{B^2 - C^2}$ in (2.18),

$$\frac{1}{2m'} = \frac{1}{2m}\frac{z^{3/2}}{15\pi^2 A}\frac{1}{(2M+x)y}\sqrt{2 - 4y^2 + \frac{5A}{2}\left(\frac{6\pi^2 x}{z^{3/2}}\right)}\sqrt{\frac{5A}{2}\left(\frac{6\pi^2 x}{z^{3/2}}\right) - 2y^2 - 2\,\Pi_{+-}(1-y^2)}. \tag{4.20}$$

The expressions (4.19) and (4.20) for the velocity and the mass of the spin waves are used in the plots of Fig. 1.

### 4.3.1 Ferromagnetic spin waves

The parameters for the ferromagnetic spin waves must fit (2.24), and are obtained from the sum of (4.7) and (4.17).

$$\begin{aligned} f_\pi^2 &= \frac{2M+x}{a^3} \\ \frac{1}{2m'} &= \frac{1}{2m}\frac{z^{3/2}}{15\pi^2 A}\frac{1}{(2M+x)}\left[-2 + \frac{5A}{2}\left(\frac{6\pi^2 x}{z^{3/2}}\right)\right], \end{aligned} \tag{4.21}$$

which corresponds to the limit of the canted parameters (4.19) taking into account that in the ferromagnetic limit $1/2m' = B$. This is plotted in Fig. 1 in the case of a ferromagnetic phase.

In this limit configuration it is particularly easy to see the effect of the charge carriers in the behavior of the spin waves. Since the interaction between the core spins is antiferromagnetic the mass derived from this interaction is negative (producing an unstable spin wave). However, the contribution from the fermionic sector compensates this sign and stabilizes the spin wave. It is also worth noticing that in this limit from the canted phase one spin wave disappears, namely, $\pi^3(u)$. Due to the existence of the remaining $U(1)$ symmetry in the ferromagnetic ground state this fluctuation does not modify the ground state any more. We can see from (4.19) that the velocity of the linear branch goes to zero smoothly in the transition to the ferromagnetic phase. This answers the question asked at the end of the

first paper in [33]: "How do the spin dynamics evolve from the double-branch state reported here into a state with only one branch characteristic of a ferromagnetic metallic phase?".

### 4.3.2 Antiferromagnetic spin waves

In this case the parameters for the effective lagrangian are obtained by summing the contributions of (4.8) and (4.18), and are given by

$$\begin{aligned} f_\pi^2 &= \frac{z}{6J_{AF}a^6} \\ v^2 &= \frac{6J_{AF}a^3M^2}{2mz}\frac{z^{3/2}}{15\pi^2 A}\frac{1}{M^2}\left[2+\frac{5A}{2}\left(\frac{6\pi^2 x}{z^{3/2}}\right)\right], \end{aligned} \tag{4.22}$$

which coincides with the limit of the parameters for the antiferromagnetic spin wave in the canted phases, $\pi^3(u)$. In the insulating phase we should take $x = 0$. This velocity is plotted in Fig. 1 for the antiferromagnetic phase.

As in the previous case we should notice the lost of one spin wave field when we carry out the limit towards the antiferromagnetic ground state, $\pi^1(u)$ (after the rotation of the reference system, $1 \to 3 \to 2$, it becomes $\pi^3(u)$). The combination of the canted phase parameters $f_\pi^2(B+C) \to 0$ with $y \to 0$. It is interesting to notice that the other remaining field, which used to be part of a ferromagnetic mode, with a quadratic dispersion relation, in the canted phase, becomes part of the antiferromagnetic spin wave with a linear dispersion relation. The remaining combination of the canted phase $f_\pi^2(B-C) \to f_3^2 v^2$ when $y \to 0$. This answers the question at the end of the previous subsection in the antiferromagnetic limit.

# 5 Disentangling Canted Phases from Phase Separation Regions

Recently controversial results have appeared in the literature regarding the existence of canted phases in doped manganites, in particular concerning their stability against phase separation [6, 23, 24, 25]. We showed in [22] that canted phases not only exist but they are also thermodynamically stable. We presented there a phase diagram where, in addition to stable canted phases, phase separation regions appear.

The phase diagram presents the following phases: antiferromagnetic insulating ($AFI$), antiferromagnetic conducting with two bands ($AFC2$), canted conducting with two bands ($CC2$), canted conducting with one band ($CC1$), ferromagnetic conducting with one band ($FC1$) and four phase separation regions between the $FC1$ phase and the remaining, i.e. $PS1$ ($AFI - FC1$), $PS2$ ($AFC2 - FC1$), $PS3$ ($CC2 - FC1$) and $PS4$ ($CC1 - FC1$).

The question of which regions the system passes through when going from the antiferromagnetic insulating phase to the ferromagnetic conducting one upon increasing the doping in the actual materials could not be satisfactorily solved there, since the answer depends critically on the values of the parameters of the model. For reasonable values of these parameters, various possibilities are allowed. We have chosen five values of the parameter $A$, in (A.11), for which the sequence of phases is the following:

$$\begin{aligned}
A = 2.20 \qquad & AFI - PS1 - FC1 \\
A = 1.75 \qquad & AFI - AFC2 - PS2 - FC1 \\
A = 1.40 \qquad & AFI - AFC2 - CC2 - PS3 - FC1 \\
A = 1.00 \qquad & AFI - AFC2 - CC2 - CC1 - PS4 - FC1 \\
A = 0.80 \qquad & AFI - AFC2 - CC2 - CC1 - FC1.
\end{aligned}$$

In order to establish differences between the canted phases and the phase separation region we must make a guess on how these phase separation regions look like, since our model does not describe these non-homogeneous regions of the phase diagram. Even though these may be very rich regions, with many different structures in them, as charge ordering, stripes, orbital ordering or polaronic excitations [25, 13, 47, 48, 49, 50, 51], we shall assume that the main structure is the coexistence of two macroscopic domains corresponding to the phases at the border of the phase separation region, and that the interphase will not disturb qualitatively the properties of each of them. With this assumption in mind we have plotted in Fig. 1 the dependence on the doping for the velocity and the mass of the spin waves for each of the values of the parameter $A$ given above.

The dotted lines corresponds to the values of the velocity and the mass in the phase separation region, for the first four values of the parameter $A$. They are constant values, because they are given by the value of the corresponding phase in the border of the phase separation region. Consider, for example, the first case, where an $AFI$ and a $FC1$ domain coexist in the phase separation region. The doping is an extensive magnitude, and even though it reduces globally over the system, the density of carriers remains constant in the $FC1$ domain, since this one reduces as the doping (considered globally) decreases.

In the third and fourth cases, where canted domains coexist with the ferromagnetic domain, we can observe two different values for the masses of the spin waves in the phase separation region, as well as one velocity.

Let us concentrate in the first versus the last case, i.e., the phase separation region with antiferromagnetic insulating and ferromagnetic conducting ($AFI - FC1$) domains versus the canted phases [6, 23, 24, 25, 52]. Since the differentiation between these two structures seems to be an experimental challenge, we describe below a few distinct properties of the

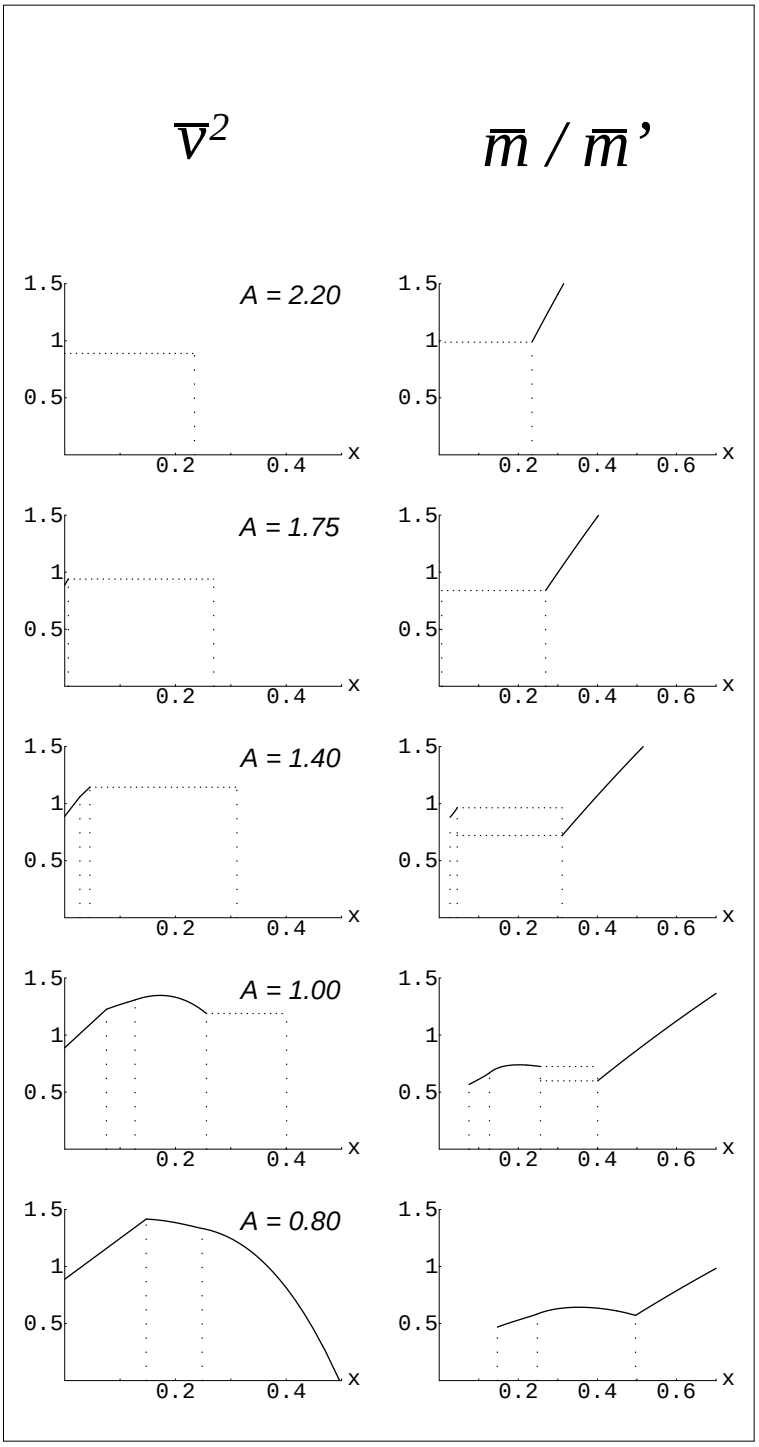


**Figure 1.** The dependence of the velocities and the masses with the doping for five different values of the parameter $A$ ($\sim t/J_{AF}$). $\bar{v}^2 = (15\pi^2 A)2mzv^2/6z^{3/2}(J_{AF}a^3M^2)$ and $\bar{m}/\bar{m}' = (15\pi^2 A)m/z^{3/2}m'$. The horizontal dotted lines correspond to the phase separation regions, and the vertical dotted lines correspond to the phase transitions.

spin waves which may help to differentiate between a canted phase and a phase separation region consisting of ferromagnetic and antiferromagnetic domains:

(i) First of all, in the canted phases dispersion relations we observe one ferromagnetic branch and one antiferromagnetic branch, whereas in the phase separation case $(F - AF)$ we should observe one ferromagnetic, but two antiferromagnetic branches.

(ii) Second, the antiferromagnetic branches present a further dramatic property: its behavior in the presence of a magnetic field along the staggered magnetization. Whereas in the antiferromagnetic case the two branches will be splitted, in the canted phase the single linear branch will not be even shifted by the presence of such a magnetic field.

(iii) Finally, we have presented in the previous section and in Fig. 1 the different behavior of the dispersion relation parameters with the doping, $A = 2.20$ for the phase separation region and $A = 0.80$ for the canted phases.

These three characteristics, in particular, the first and the second one which are of rather general nature (model independent), should allow to experimentally differentiate the regions of the phase diagram where ferromagnetic and antiferromagnetic phases coexist from those where real canted phases exist.

# 6 Conclusions

We have presented a complete study of the spin waves in canted phases. We have exploited the spontaneous symmetry breaking pattern $SU(2) \to 1$ to construct an effective lagrangian for low energy and momentum spin waves in canted phases at next to leading order. For simplicity, we have chosen a cubic lattice, but any other lattice can be treated within the same formalism. The lagrangian at leading order depends on five parameters and to next to leading on nine. The leading lagrangian yields two spin wave modes, one with a quadratic and one with a linear dispersion relation. The leading effective lagrangians for ferromagnetic and antiferromagnetic ground states were also considered as limit cases of the canted configuration. These depend on two parameters only.

Since the canted phases appear in doped manganites, and are associated with conducting properties of these materials we have also presented interaction lagrangians of spin waves with charge carriers. Whereas the lagrangian for spin waves alone is of general nature (model independent), the interaction with charge carriers depends on microscopic features of the material, in particular on the number of conducting bands available. We have chosen a simple case (two band) which is inspired in a realistic model introduced in [22] for the study of the phase diagram of doped manganites. Again we have derived the interaction lagrangian

for ferromagnetic and antiferromagnetic phases as the extreme cases of the interaction with canted spin waves.

We have applied our results to the study of the spin waves in doped manganites using the continuum double exchange model [22]. We obtained the explicit dependence on the doping and the canting angle for $f_\pi$, $1/2m'$, $f_3$ and $v$, which determine the dispersion relations for the spin waves, and we have plotted them in Fig. 1 for several parameters.

Finally, we have proposed three ways to tell experimentally apart canted phases from phase separation regions (coexistence of ferromagnetic and antiferromagnetic phases) by looking at suitable properties of spin waves. The results above may also be useful for a more refined study of the phase diagram of doped manganites. In particular the leading quantum corrections to the classical spin dynamics in the low energy region are due to spin waves. It would be very interesting to elucidate the effect of these corrections in the phase diagram.

# Acknowledgments

J.M.R. thanks Daniel Sánchez-Portal and Eduardo Fradkin for illuminating discussions. We thank also M. Hennion for bringing to our attention ref. [33]. J.M.R. is supported by a Basque Government F.P.I. postdoctoral fellowship. Financial support from NSF, grant no. DMR98-17941, from CICYT (Spain), contract AEN98-0431 and from CIRIT (Catalonia), contract 1998SGR 00026 is also acknowledged.

# Appendix A: Vacuum Polarization Tensor

The vacuum polarization tensor, as was defined in subsection 4.2 reads

$$\Pi_{ab}^{(i,j)}(p) = -i \int \frac{dq}{(2\pi)^4} \, (p+q)^i L_{1a}^{-1}(p+q) \, q^j L_{1b}^{-1}(q), \tag{A.1}$$

where

$$L_{1a}^{-1}(q) = \frac{1}{\omega - \dfrac{\mathbf{k}^2}{2m} - \Omega_a + i\eta\omega} \quad , \quad \Omega_\pm = -\frac{|J_H|M}{2}\sqrt{1+\gamma^2 \pm 2\gamma\cos\frac{\theta}{2}} - \mu. \tag{A.2}$$

The symmetry properties of this tensor under the change of sign of the energy and momentum are given by

$$\begin{aligned} \Pi_{ab}^{(i,j)}(-\nu,\mathbf{p}) &= (-1)^{\delta_{0i}+\delta_{0j}} \, \Pi_{ba}^{(j,i)}(\nu,\mathbf{p}) \\ \Pi_{ab}^{(i,j)}(\nu,-\mathbf{p}) &= (-1)^{\delta_{0i}+\delta_{0j}} \, \Pi_{ab}^{(i,j)}(\nu,\mathbf{p}) \\ \Pi_{ab}^{(i,j)}(-\nu,-\mathbf{p}) &= \Pi_{ba}^{(j,i)}(\nu,\mathbf{p}). \end{aligned} \tag{A.3}$$

In order to simplify the calculation of the integrals we chose a reference system with its third component parallel to the external momentum in $\Pi_{ab}^{(i,j)}(\nu,\mathbf{p})$, namely,

$$\hat{\mathbf{e}}_{(1)} = \frac{(\hat{\mathbf{p}}\hat{\mathbf{k}})\hat{\mathbf{p}} - \hat{\mathbf{k}}}{|\hat{\mathbf{k}}\times\hat{\mathbf{p}}|} \quad , \quad \hat{\mathbf{e}}_{(2)} = \frac{\hat{\mathbf{k}}\times\hat{\mathbf{p}}}{|\hat{\mathbf{k}}\times\hat{\mathbf{p}}|} \quad , \quad \hat{\mathbf{e}}_{(3)} = \hat{\mathbf{p}}, \tag{A.4}$$

where $\hat{\mathbf{k}}$ is a unit vector in the third crystallographic direction.

We will denote the components of the vectors and tensors in the new basis with Greek indices, instead of Latin ones, such that they verify $w_\alpha = w_i\ e^i_{(\alpha)}$, and consequently,

$$\Pi_{ab}^{(\alpha,\beta)}(p) = \Pi_{ab}^{(i,j)}(p)\ e^i_{(\alpha)} e^j_{(\beta)}. \tag{A.5}$$

Therefore the symmetry properties under the change of sign of the energy and momentum in the new basis become

$$\begin{aligned}
\Pi_{ab}^{(\alpha,\beta)}(-\nu,\mathbf{p}) &= (-1)^{\delta_{0\alpha}+\delta_{0\beta}}\ \Pi_{ba}^{(\beta,\alpha)}(\nu,\mathbf{p}) \\
\Pi_{ab}^{(\alpha,\beta)}(\nu,-\mathbf{p}) &= (-1)^{\delta_{0\alpha}+\delta_{0\beta}+\delta_{1\alpha}+\delta_{1\beta}}\ \Pi_{ab}^{(\alpha,\beta)}(\nu,\mathbf{p}) \\
\Pi_{ab}^{(\alpha,\beta)}(-\nu,-\mathbf{p}) &= (-1)^{\delta_{1\alpha}+\delta_{1\beta}}\ \Pi_{ba}^{(\beta,\alpha)}(\nu,\mathbf{p}).
\end{aligned} \tag{A.6}$$

In this basis, after some straightforward algebra, following [46], it is easy to see that all the dependence on the components $q^1$ and $q^2$ of the integrand in (A.1) comes from the explicit dependence $(p+q)^\alpha$ and $q^\beta$, and therefore it is verified that

$$\begin{aligned}
\Pi_{ab}^{(0,\alpha)}(p) &= \delta^{\alpha 3}\ \Pi_{ab}^{(0,3)}(p) \\
\Pi_{ab}^{(\alpha,\beta)}(p) &= \delta^{\alpha\beta}\ \Pi_{ab}^{(\alpha,\alpha)}(p),
\end{aligned} \tag{A.7}$$

where the repeated indices are not summed.

Once the symmetry properties of the vacuum polarization tensor have been considered we will address its calculation. As it was stated in the subsection 4.2 it is enough to calculate the limit $p^\mu \to 0$ of the tensor, i.e. $\Pi_{ab}^{(i,j)}(0)$, to obtain the leading contribution to the effective lagrangian. Since the external energy, $\nu$, and momentum, $\mathbf{p}$, injected in the fermionic loop, are related, this limit must be taken carefully. If they correspond to a $\pi^3(x)$ spin wave their relation is linear, $\nu \sim |\mathbf{p}|$, while the relation for $\pi^\pm(x)$ is quadratic, $\nu \sim \mathbf{p}^2$. The tensor components are given by

$$\begin{aligned}
\Pi_{aa}^{(0,0)}(0) &= \frac{mk_a}{4\pi^2}\left[-2 + x_a \log\left|\frac{1+x_a}{1-x_a}\right| - i\pi|x_a|\theta(1-|x_a|)\right]\theta(-\Omega_a) \quad , \quad x_a = \frac{m\nu}{k_a|\mathbf{p}|} \\
\Pi_{aa}^{(0,3)}(0) &= \frac{m\nu}{|\mathbf{p}|}\ \Pi_{aa}^{(0,0)}(0) \\
\Pi_{aa}^{(1,1)}(0) &= \Pi_{aa}^{(2,2)}(0) = \frac{mk_a^3}{12\pi^2}\ \theta(-\Omega_a) + \frac{1}{2}k_a^2(1-x_a^2)\ \Pi_{aa}^{(0,0)}(0)
\end{aligned} \tag{A.8}$$

$$\Pi^{(3,3)}_{aa}(0) = -\frac{mk_a^3}{6\pi^2}\,\theta(-\Omega_a) + \left(\frac{m\nu}{|\mathbf{p}|}\right)^2 \Pi^{(0,0)}_{aa}(0)$$
$$\Pi^{(\alpha,\alpha)}_{+-}(0) = -\frac{m}{15\pi^2}\,\frac{k_+^5\theta(-\Omega_+) - k_-^5\theta(-\Omega_-)}{k_+^2 - k_-^2} = -\frac{mJ_{AF}M^2}{t}\,\Pi_{+-} \quad , \quad (\alpha = 1,2,3),$$

where $k_a = \sqrt{-2m\Omega_a}$ represents the Fermi momentum in each band $a = +,-$, and $x_a$ is the relation between the spin wave velocity and the Fermi velocity in each band. The step functions $\theta(-\Omega_a)$ ensures that only the bands which are bellow the chemical potential contribute to the result. In the expressions above the summation convention was not used. An interesting result arises from considering the summation over $\Pi^{(3,3)}_{aa}(0)$, namely,

$$\begin{aligned}\sum_a \Pi^{(3,3)}_{aa}(0) &= -m\frac{(2m)^{3/2}}{6\pi^2}\sum_a(-\Omega_a)^{3/2}\theta(-\Omega_a) + \left(\frac{m\nu}{|\mathbf{p}|}\right)^2 \sum_a \Pi^{(0,0)}_{aa}(0) \\ &= -\frac{mx}{a^3} + \left(\frac{m\nu}{|\mathbf{p}|}\right)^2 \sum_a \Pi^{(0,0)}_{aa}(0), \end{aligned} \tag{A.9}$$

as can be verified from an explicit calculation of the integral which gives the doping $x$ in (4.10).

The results obtained until now are exact (in the limit of $p^\mu \to 0$). In order to obtain further analytic results for $\Pi^{(\alpha,\alpha)}_{+-}(0)$ in (A.8) we will use the value of $\Omega_\pm$ to leading order in $\gamma$, already obtained in [22],

$$\Omega_\pm = -t(y_0 \pm y), \tag{A.10}$$

where $y_0$ is a measure of the chemical potential.

In the $CC1$ phase we obtained in [22] the following values for the canting angle, $y$, and the doping, $x$:

$$y = \frac{5}{8}A(y_0+y)^{3/2} = \frac{5}{8}A\left(\frac{6\pi^2 x}{z^{3/2}}\right) \qquad , \qquad A = \frac{z^{3/2}}{15\pi^2}\frac{t}{J_{AF}a^3M^2}, \tag{A.11}$$

and therefore

$$CC1: \qquad \Pi_{+-} = \frac{a^3A}{z^{3/2}}\,\frac{k_+^5}{k_+^2-k_-^2}\,\theta(-\Omega_+) = \frac{4}{5}\left(\frac{6\pi^2x}{z^{3/2}}\right)^{2/3}. \tag{A.12}$$

The calculation is a little bit more complicated in the two band case, $CC2$, where we obtained in [22] for $y$ and $x$ the following expressions:

$$\begin{aligned} y &= \frac{5}{8}A\left[(y_0+y)^{3/2} - (y_0-y)^{3/2}\right] \\ \frac{5}{4}A(y^2+3y_0^2) &= (y_0+y)^{3/2} + (y_0-y)^{3/2} = \frac{6\pi^2x}{z^{3/2}}, \end{aligned} \tag{A.13}$$

which yields after eliminating the chemical potential measure, $y_0$,

$$CC2: \quad \Pi_{+-} = \frac{a^3 A}{z^{3/2}} \frac{k_+^5 \theta(-\Omega_+) - k_-^5 \theta(-\Omega_-)}{k_+^2 - k_-^2} = \\ = \frac{1}{\sqrt{3}} \frac{4}{5} \sqrt{\frac{4}{5A}\left(\frac{6\pi^2 x}{z^{3/2}}\right) - y^2} + \frac{A}{2}\left(\frac{6\pi^2 x}{z^{3/2}}\right) \stackrel{y\to 0}{\longrightarrow} \frac{5A}{4}\left(\frac{6\pi^2 x}{z^{3/2}}\right), \quad \text{(A.14)}$$

where the limit $y \to 0$ can be taken smoothly, and the previous result is obtained by taking into account that $A y_0^{1/2} = 8/15$ when $y = 0$.

# References


[1] S. Sachdev and T. Senthil, *Ann. Phys. (N.Y.)* **251** (1996) 76.

S. Das Sarma, S. Sachdev and L. Zheng, *Phys. Rev.* **B58** (1998) 4672;

[2] G. H. Jonker and J. H. Van Santen, *Physica* **50** (1950) 337.

[3] P. W. Anderson and H. Hasegawa, *Phys. Rev.* **100** (1955) 675.

[4] P. G. De Gennes, *Phys. Rev.* **118** (1960) 141.

[5] C. Zener, *Phys. Rev.* **82** (1951) 403.

[6] D. P. Arovas and F. Guinea, *Phys. Rev.* **B58** (1998) 9150.

[7] A. J. Millis, P. B. Littlewood and B. I. Shraiman, *Phys. Rev. Lett.* **75** (1995) 5144.

[8] L.-J. Zou, Q.-Q. Zheng and H. Q. Lin, *Phys. Rev.* **B56** (1997) 13669.

[9] R. Maezono, S. Ishihara and N. Nagaosa, *Phys. Rev.* **B58** (1998) 11583.

[10] D. I. Golosov, M. R. Norman and K. Levin, *Phys. Rev.* **B58** (1998) 8617.

[11] H. Aliaga, R. Allub and B. Alascio, *Solid State Commun.* **110** (1999) 525.

[12] N. Furukawa, *Thermodynamics of the Double Exchange Model*, cond-mat/9812066. To be published in Proc. Conference on Physics of Manganites (July 1998 at Michigan State University).

[13] R. Y. Gu, Z. D. Wang, S.-Q. Shen and D. Y. Xing, *Phase diagram of an extended Kondo lattice model for manganites: the Schwinger-boson mean-field approach*, cond-mat/9905152.

[14] W. E. Pickett and D. J. Singh *Phys. Rev.* **B53** (1996) 1146.

[15] A. S. Alexandrov and A. M. Bratkovsky, *J. Phys.: Cond. Matter* **11** (1999) 1989.

[16] D. M. Edwards, A. C. M. Green and K. Kubo, *J. Phys.: Cond. Matter* **11** (1999) 2791.

[17] M. O. Dzero, L. P. Gor'kov and V. Z. Kresin, *Solid State Commun.* **112** (1999) 707.

[18] M. Jaime, P. Lin, M. B. Salamon and P. D. Han, *Phys. Rev.* **B58** (1998) R5901;

S. H. Chun, M. B. Salamon, Y. Lyanda-Geller, P. M. Goldbart and P. D. Han, *Phys. Rev. Lett.* **84** (2000) 757;

M. Jaime and M. B. Salamon, *Electronic Transport in La-Ca Manganites* cond-mat/9902284. To be published in the proceedings of the Workshop on Physics of Manganites, MSU, July 1998

[19] O. Zachar, A. M. Tsvelik, *One-dimensional electron gas interacting with a Heisenberg spin-1/2 chain*, cond-mat/9909296.

[20] A. P. Ramirez, *J. Phys.: Cond. Matter* **9** (1997) 8171.

J. M. D. Coey, M. Viret and S. von Molnar, *Adv. in Phys.* **40** (1999) 167.

[21] L. Sheng, D. N. Sheng, C. S. Ting, *Phys. Rev.* **B59** (1999) 13550;

P. Raychaudhuri, C. Mitra, A. Paramekanti, R. Pinto, A. K. Nigam and S. K. Dhar, *J. Phys.: Cond. Matter* **10** (1998) L191.

[22] J. M. Román and J. Soto, *Phys. Rev.* **B59** (1999) 11418.

[23] D. P. Arovas, G. Gómez-Santos and F. Guinea, *Phys. Rev.* **B59** (1999) 13569.

[24] M. Yu. Kagan, D. I. Khomskii and M. V. Mostovoy, *European Physical Journal* **B12** (1999) 217.

[25] E. Dagotto, S. Yunoki and A. Moreo, *Phase separation in models for manganites: theoretical aspects and comparation with experiments*, cond-mat/9809380. To appear in proceedings of the workshop "Physics of Manganites", Michigan State University, July 26–29, 1998, eds. by T. A. Kaplan and S. D. Mahanti, Plenum Publishing Corporation;

S. Yunoki, A. Moreo and E. Dagotto, *Phys. Rev. Lett.* **81** (1998) 5612;

A. Moreo, S. Yunoki and E. Dagotto, *The Phase Separation Scenario for Manganese Oxides*, cond-mat/9901057. To be published in *Science*.

[26] Y. Matsushita, R. Shiina and C. Ishii, *Solid State Commun.* **97** (1996) 71.

[27] R. Maezono and N. Nagaosa, *Phys. Rev.* **B61** (2000) 1189.

[28] J. Loos and H. Fehske, *Physica* **B259-261** (1999) 801.

[29] R. Y. Gu, Shun-Qing Shen, Z. D. Wang and D. Y. Xing, *Linear spin and orbital wave theory for undoped manganites*, cond-mat/9908464.

[30] M. B. Fontes, J. C. Trochez, B. Giordanengo, S. L. Bud'ko, D. R. Sanchez, E. M. Baggio-Saitovitch and M. A. Continentino, *Phys. Rev.* **B60** (1999) 6781.

[31] D. I. Golosov, *Spin Wave Theory of Double Exchange Magnets*, cond-mat/9909213.

[32] I. R. Pimentel, F. Carvalho, L. M. Martelo and R. Orbach, *Phys. Rev.* **B60** (1999) 12329.

[33] F. Moussa, M. Hennion, G. Biotteau, J. Rodríguez-Carvajal, L. Pinsard and A. Revcolevschi, *Phys. Rev.* **B60** (1999) 12299;

M. Hennion, F. Moussa, G. Biotteau, J. Rodríguez-Carvajal, L. Pinsard and A. Revcolevschi, *Phys. Rev.* **B61** (2000) 9513.

[34] J. Goldstone, *Nuovo Cim.* **19** (1961) 145.

[35] G. S. Guralnik, C. R. Hagen and T. W. B. Kibble, *Advances in particle physics*, Vol.2, p.567, ed. R. L. Cool and R. E. Marshak (Willey, New York, 1968).

[36] S. Coleman, J. Wess and B. Zumino, *Phys. Rev.* **177** (1969) 2239;

C. Callan, S. Coleman, J. Wess and B. Zumino, *Phys. Rev.* **177** (1969) 2247.

[37] J. Gasser and H. Leutwyler, *Ann. Phys. (N.Y.)* **158** (1984) 142.

[38] H. Leutwyler, *Phys. Rev.* **D49** (1994) 3033.

[39] J. M. Román and J. Soto, *Int. J. Mod. Phys.* **B13** (1999) 755.

[40] C. P. Burgess, *Goldstone and Pseudo-Goldstone bosons in Nuclear, Particle and Condensed Matter Physics*, hep-th/9808176.

[41] J. M. Román and J. Soto, *Ann. Phys. (N.Y.)* **273** (1999) 37.

[42] C. P. Hofmann, *Thermodynamic Behavior of the $O(3)$ Ferromagnet*, Universität Bern, preprint no. BUTP-97/31;

C. P. Hofmann, *Phys. Rev.* **B60** (1999) 388;

C. P. Hofmann, *Phys. Rev.* **B60** (1999) 406.

[43] H. B. Nielsen and S. Chada, *Nucl. Phys.* **B105** (1976) 445.

[44] J.F. Donoghue, E. Golowich and B.R. Holstein, *Dynamics of the Standard Model* (Section **IV-7**), (Cambridge University Press, 1992).

[45] E. Fradkin, *Field Theories of Condensed Matter Systems* (Addison-Wesley, Reading, MA, 1990);

S. Chakravarty, B. I. Halperin and D. R. Nelson, *Phys. Rev.* **B39** (1989) 2344.

[46] A. L. Fetter and J. D. Walecka, *Quantum Theory of Many-Particle Systems*, (McGraw-Hill, New York, 1971).

[47] S. Yunoki, T. Hotta and E. Dagotto, *Ferromagnetic, A-type, and Charge-Ordered CE-type States in Doped Manganites using Jahn-Teller Phonons*, cond-mat/9909254.

[48] T. Mutou and H. Kontani, *Phys. Rev. Lett.* **83** (1999) 3685.

[49] L. Sheng and C. S. Ting, *Modified Double Exchange Model with Novel Spin and Orbital Coupling: Phase Diagram of The Manganites*, cond-mat/9812374;

J. van den Brink and D. Khomskii, *Phys. Rev. Lett.* **82** (1999) 1016.

[50] P. Benedetti and R. Zeyher, *Phys. Rev.* **B59** (1999) 9923;

T. Hotta, S. Yunoki and E. Dagotto, *Cooperative Jahn-Teller Effect on the Magnetic Structure of Manganese Oxides*, cond-mat/9907430. To appear in proceedings of the conference "Science and Technology of Magnetic Oxides '99", La Jolla, July 5–7, 1999.

[51] T. Mizokawa, D. I. Khomskii and G. A. Sawatzky, *Phys. Rev.* **B60** (1999) 7309.

[52] A. Biswas, M. Rajeswari, R. C. Srivastava, Y. H. Li, T. Venkatesan, R. L. Greene and A. J. Millis, *Phys. Rev.* **B61** (2000) 9665.